Journal of Environmental Management 380 (2025) 124915

Contents lists available at ScienceDirect

Journal of Environmental Management

journal homepage: www.elsevier.com/locate/jenvman

Research article

Mapping the distribution and condition of mountain peatlands in Colombia for sustainable ecosystem management

Patrick Nicolás Skillings-Neira [a,*], Juan C. Benavides [b], Michael J. Battaglia [c], Rodney A. Chimner [a], Laura Bourgeau-Chavez [c], Craig Wayson [d], Randall Kolka [e], Erik A. Lilleskov [f]

[a] Michigan Technological University, College of Forest Resources and Environmental Science Houghton, MI, USA
[b] Department of Ecology and Territory, Faculty of Environmental and Rural Studies, Pontificia Universidad Javeriana, Bogotá, Colombia
[c] Michigan Technological University, Michigan Tech Research Institute Ann Arbor, MI, USA
[d] USDA Forest Service International Programs, Washington D.C, USA
[e] USDA Forest Service Northern Research Station, Grand Rapids, MN, USA
[f] USDA Forest Service Northern Research Station, Climate, Fire and Carbon Cycle Sciences Unit, Houghton, MI, USA

ARTICLE INFO

Keywords:
Andes
Peatlands
Páramos
Soil carbon
Remote sensing
Disturbance
National map

ABSTRACT

High mountain peatlands in Colombia play a crucial role in water regulation, store significant carbon, and yet remain poorly studied and threatened. The lack of a comprehensive national peatland map hinders effective management. Our objectives were to create a national mountain peatland map for Colombia, assess peatland distribution, quantify degraded pasture peatlands, and evaluate soil carbon percentages and bulk density in the top 40 cm of mountain peatlands soils. We developed and compared three national-scale maps using field validation, Sentinel-2 imagery, SAR data, and topographic variables as inputs to a Random Forest classifier, each reflecting a different grouping of the study area. The Subregional map classifies four smaller subregions individually and merges them, the Regional groups two larger regions, and the National classifies the entire study area. Mapping 4.8 million hectares, we found peatlands occupy approximately 225,000 to 250,000 ha. About 13–15% are pasture peatlands, even within protected areas, 7–8% have been disturbed. Soil analyses up to 40 cm show consistently high carbon percentage in undisturbed peatlands, whereas pasture peatlands exhibit lower carbon and higher bulk density, revealing detrimental effects caused by drainage and livestock. These findings underscore the urgent need for targeted conservation and restoration to reduce greenhouse gas emissions, protect water resources, and strengthen climate mitigation strategies. Future research should refine peatland depth estimates to enhance the accuracy of peatland carbon stock assessments, leverage all three maps to improve training data in areas with substantial discrepancies, and use emerging technologies to better detect unaccounted peatland degradation.

1. Introduction

Peatlands cover only 3–4% of the world's land surface but store one-third of global soil carbon, estimated at 450,000 to 650,000 million tons (UNEP, 2022). Undisturbed peatlands act as long-term net carbon sinks, but degradation can convert them into net sources of greenhouse gases (GHG) estimated at over four percent of human-caused emissions (UNEP, 2022). Mapping peatlands reveals their distribution, helps calculate soil carbon stocks, and allows evaluation of their potential risk of degradation (Chimner et al., 2023; Gutiérrez-Díaz et al., 2020; Hribljan et al., 2015, 2016). This has led to worldwide initiatives to map peatlands (Gumbricht et al., 2017; Melton et al., 2022; UNEP, 2022; Xu et al., 2018), reflecting their importance for climate change mitigation and conservation efforts. While global peatland mapping efforts have made significant progress, gaps persist due to a range of challenges in accurately mapping peatlands.

The Global Peatland Assessment 2.0 (GPA2) provides the most comprehensive global peatland map to date, identifying 500 million ha of peatlands globally, predominantly distributed in Asia (33%), North America (32%), Latin America and the Caribbean (13%), Europe (12%), and Africa (8%) (Greifswald Mire Centre, 2022; UNEP, 2022). The GPA2

* Corresponding author.
E-mail address: pnskilli@mtu.edu (P.N. Skillings-Neira).

https://doi.org/10.1016/j.jenvman.2025.124915
Received 14 October 2024; Received in revised form 3 March 2025; Accepted 7 March 2025

Abbreviations

GHG -	Greenhouse Gases
GPA2 -	The Global Peatland Assessment 2.0
GPM2 -	Global Peatland Map 2.0
LAC -	Latin America and the Caribbean
SAR -	Synthetic Aperture Radar
DEM -	Digital Elevation Model
NAT –	National map
REG –	Regional map
SREG –	Subregional map
SNS -	Sierra Nevada de Santa Marta
NEC -	Northeastern Cordillera
SEC -	Southeastern Cordillera
NAR -	Nariño-Putumayo
CC_WC -	Central and Western Cordilleras
LULC -	Land Use and Land Cover
GEE -	Google Earth Engine
OM -	Organic Matter
BD -	Bulk Density
%C -	Carbon Percentage
TPI -	Topographic Position Index
SRTM -	Shuttle Radar Topography Mission
NDVI -	Normalized Difference Vegetation Index
GRD -	Ground Range Detected
RF -	Random Forest
NWMC -	National Wetland Map of Colombia
NLCMC -	National Land Cover Map of Colombia

highlights that 88% of existing peatlands are conserved. However, if GHG emissions from drained and degraded peatlands persist at the current rate until 2100, their impact on the global emissions budget will constitute 41% of the emissions needed to keep global warming below 1.5 °C (UNEP, 2022). Despite advancements like the Global Peatland Map 2.0 (GPM2) many regions remain underrepresented due to limitations in detecting smaller peatlands, incomplete national-scale data, and ineffective models for unique environmental conditions (Gumbricht et al., 2017; Melton et al., 2022; UNEP, 2022; Xu et al., 2018).

Specifically, in Latin America and the Caribbean (LAC), mapping effort predominantly focuses on larger and lower elevation peatlands leading to a systemic underrepresentation of mountain peatlands, particularly in the northern Andes. For instance, the GPM2 estimates that only 2% of peatlands mapped in LAC are located in tropical mountain systems (Greifswald Mire Centre, 2022). Other global studies have failed to map any peatlands in the Andes due to model limitations in capturing mountain peatlands (Gumbricht et al., 2017; Melton et al., 2022; Xu et al., 2018). However, recent regional studies in the northern Andes, covering areas between 250,000–400,000 ha, reveal that peatlands might constitute 6%–18% of these regions (Battaglia et al., 2024; Chimner et al., 2019; Hribljan et al., 2017). This highlights the need for more dedicated mapping efforts to capture mountain peatlands distribution.

Mountain peatlands play a crucial role in the regional carbon budget due to their significant peat deposits (Chimner et al., 2023; Cooper et al., 2015; Hribljan et al., 2015, 2016, 2024). The humid tropical Andes climate and unique topography promote peat accumulation in poorly drained valleys, slopes, and geomorphological depressions (Cooper et al., 2019). These peatlands are characterized by dense soils, composed of a mix of mineral sediments and organic matter from geologically active basins (Cooper et al., 2019; UNEP, 2022). In most cases, tropical mountain peatlands accumulate more organic carbon per unit area than peatlands at higher latitudes, reaching depths of up to 11 m (Cooper et al., 2015; Hribljan et al., 2024). Additionally, peatland's high water-retention capacity is also vital for regulating water flow and runoff (Hofstede et al., 2023; Lazo et al., 2019; Mosquera et al., 2015), safeguarding lower elevation communities from climate hazards like El Niño (Galvis et al., 2021; Hofstede et al., 2023).

Mapping peatlands in the northern Andes presents significant challenges. Accurate mapping is difficult because of the small size of individual peatlands, high diversity of wetland types, and high similarity of vegetation in peatland and non-peatland areas (Battaglia et al., 2024; Bourgeau-Chavez et al., 2018; Hribljan et al., 2017). Persistent cloud cover and a lack of comprehensive field data also hinder large-scale mapping (Bourgeau-Chavez et al., 2018; Hribljan et al., 2017; UNEP, 2022; Xu et al., 2018).

Despite these challenges, regional efforts in páramos of Ecuador and Colombia (Battaglia et al., 2024; Hribljan et al., 2017), and the puna of Peru (Chimner et al., 2019) have advanced mountain peatland mapping. These mapping efforts used a combination of field validation, topographic information, multispectral imaging, and Synthetic Aperture Radar (SAR) for their classification. Multispectral imagery is crucial for classifying vegetation types, but it faces challenges in distinguishing between wetland and upland areas within páramos due to similar vegetation composition. SAR data has been effective in mapping wetlands, with both L and C band sensors playing a key role in detecting soil moisture and differences in vegetation structure (Bourgeau-Chavez et al., 2015, 2018). Temporal analysis of SAR imagery allows for comparing conditions across wet and dry seasons, distinguishing between peatlands, which have stable water tables in both wet and dry seasons, and mineral wetlands or other upland areas, which tend to be more variable (Battaglia et al., 2024). Additionally, a digital elevation model (DEM) is employed to obtain topographic data. While elevation data is not used directly for classification, it proves useful in generating topographic indexes and slope layers. These are particularly valuable in peatland detection, allowing for the differentiation between flat terrains, valleys and depressions, and convex surfaces, which is instrumental in classifying peatlands.

High mountain peatlands in Colombia, located within the páramos—a biome between the Andean treeline and the periglacial zone—face significant ecological challenges. Although Colombia's Law 1930, enacted in 2018, mandates the sustainable management and protection of páramos by restricting activities to low-impact agriculture, it does not specifically prohibit peatland disturbance (Congreso de Colombia, 2018) Mountain peatland disturbance leads to substantial greenhouse gas emissions and disrupts water storage and supply (Benavides, 2014; Krause et al., 2021; Planas Clarke et al., 2020; Roucoux et al., 2017). Despite 51% of páramo regions being under a category of protection, 15% have undergone significant transformation due to the economic activities of about 80,000 páramo inhabitants who rely primarily on grazing and potato and onion farming in Colombia (DANE, 2020; Galvis et al., 2021; Galvis et al., 2021). Agricultural activities often involve draining peatlands to simplify access or utilize organic-rich soils in flatter areas. Quantifying the extent and degradation of peatlands converted to pasture is crucial for identifying priority areas for conservation and restoration. Since these areas can rapidly release carbon into the atmosphere, detailed assessments of their size and condition are necessary.

The absence of comprehensive peatland mapping at a national level in Colombia hampers effective environmental management and policy formulation, because information on their total area, location, and condition of peatlands is used by managers for decisions on appropriate land uses. This information is also important to decision-makers setting policies such as nationally determined contributions to the Paris Agreement, because quantitative estimates of peatland area and activity data are foundational inputs to calculations of potential climate benefits of land use change.

To address this need, the main objectives of this research were to create the first ground-truthed national mountain peatland map of Colombia, assess mountain peatland abundance and distribution, identify transformed peatland areas that are used as pastures and undergoing degradation, and quantify soil carbon content and bulk density in the top 40 cm of mountain peatlands soils. In addition to these goals, we address the question: what differences emerge in peatland classification results and distribution when using different spatial extents in the classifiers, and what is the most effective spatial extent for mapping peatlands in Colombia? The spatial extent refers to the size of the geographic areas used in combination with the corresponding training data when running our classifier. To address this question, we generated three maps: National (NAT), Regional (REG), and Subregional (SREG). The SREG map combines the classification results from independent runs on four subregions of the study area to generate the national map. The REG map merges the results from independent runs on two regions, each formed by combining two of the initial subregions. The NAT map represents the classification result from an independent run on the entire study area. This methodology is transferable to other mountainous regions and is of broad interest to peatland scientists and managers globally.

2. Methodology

2.1. Study area

Colombia's high mountain peatlands are found across the páramos, covering the isolated Sierra Nevada de Santa Marta (SNS) and the Eastern, Central, and Western Andean Mountain ranges, also known as cordilleras (Fig. 1). The geomorphology, combined with the páramos' cold, humid climate, create optimal conditions for peatland formation. Humid air currents from the oceans and the Amazon, shaped by the Intertropical Convergence Zone, deliver abundant rainfall, particularly to windward slopes (Castaño and Franco-Vidal, 2003). The climate results in a gradient of páramo environments, ranging from dry to superhumid, with annual precipitation varying from 600 mm to over 4000 mm (Rangel-Ch, 2000).

Our research was conducted on approximately 4.8 million ha in the northern Andes, above an elevation of 2750 masl and extending 30 km beyond Colombia's national borders (Fig. 1). The geographical selection criteria serves multiple research purposes. It includes continuous páramo ecosystems that Colombia shares with Venezuela (Páramo de Tamá and La Serranía del Perijá) and Ecuador (Páramo de Chiles and the Reserva Ecológica El Ángel), contains all known páramo areas extending down to an elevation of 2750 and covers disturbed peatlands which, despite agricultural conversion into pastures, can still be detected at elevations above 2750 m. A few isolated small polygons equal to or less than 200 ha were removed from the study area, as they predominantly consisted of small ridges or mountain tops, with no peatlands. Moreover, a portion of the Southeastern cordillera (57,400 ha, or 1.2 % of the area above 2750 m) was omitted from the analysis owing to the scarcity of cloud-free images and the logistic challenges to obtaining field data (Fig. 1).

Building on the delineated study area, this research undertakes a multi-level spatial extent classification assessment. Three classification maps (SREG, REG, NAT) are produced at different spatial extents. The SREG map combines individual classification results of four specific subregions: the Northeastern Cordillera (NEC), the Southeastern Cordillera (SEC), Nariño-Putumayo (NAR), and the combined Central and Western Cordilleras (CC_WC) (Fig. 1). Intentional overlaps between NEC and SEC, as well as NAR and CC_WC, are designed to enhance models by reusing training and validation data in these overlapping areas. The REG map merges these pairs of subregions into two broader regions: NEC_SEC and NAR_CC_WC. Meanwhile, the National extent covers the entire study area, including the SNS, where field data collection was precluded by logistical challenges.

2.2. Data collection

To create the classification maps, it was necessary to have two types of data sources: the training and validation polygons for the model, and our image stack, which consist of a set of layers we processed from various remote sensors images (Fig. 2).

2.2.1. Training and validation polygons

For the creation of classification maps, a shapefile containing polygons for training and validation was produced. These polygons, delineated on the input image stack, were used to select pixels that represent sites with known land use and land cover (LULC) classes. For training, pixels were randomly sampled from polygons in proportion to their area, up to 500 per class; if a class had few polygons, only the available pixels were used. Validation included all pixels within the validation polygons to assess accuracy. The dataset comprises 4242 polygons drawn from diverse sources of georeferenced information that provided specifics on location and land cover. Of these, 2240 polygons were drawn using image interpretation of high-resolution imagery from Google Earth, Google Street View, or a selected combination of Sentinel 2 bands within our image stack, enhancing the interpretation of LULC classes. This approach facilitated the identification of various LULC classes. However, the reliance on satellite imagery for initial classification had limitations, especially in accurately distinguishing mineral wetlands and peatland types and refining other LULC classes, which led to the necessity of field verification.

A total of 2002 polygons were delineated with field verification data obtained from multiple sources. Our primary source of field verification consisted of extensive field visits conducted from April 2019 to March 2023. Secondary sources included interpretation of drone images taken during these field visits, a review of peatland literature offering georeferenced site descriptions (Benavides et al., 2023; Cataño Díaz et al., 2014; Urbina and Benavides, 2015; Villa et al., 2019), a field database from Ecuadorian colleagues involved in peatland mapping (specifically from the *Reserva el Angel*, which borders the páramo of Chiles in Colombia), and personal communications with experts possessing first-hand knowledge of peatlands within the study area (see Supplementary Material-Figure S1 for more details).

2.2.1.1. Primary field verification methods. Over the course of four years, our field visits necessitated an adaptable and evolving approach to site selection, driven by the unique logistical requirements essential for maintaining safe working conditions for our field crew. Our study used the approach of (Battaglia et al., 2024) where we created a preliminary weakly supervised classification in which potential wetland and upland areas were classified using visual analysis of aerial and satellite imagery from Google Earth, identifying likely peatland and upland points. These points were buffered by 20 m to form training polygons for a Random Forest classifier (Breiman, 2001), incorporating remote sensing data and imagery from Landsat 8 and Sentinel-1 C-band SAR via Google Earth Engine (GEE) to create classified maps containing two classes: Potential wetlands and uplands. Subsequently, potential field sites were determined through a random sampling strategy constrained by accessibility from roads using an Open Street Maps layer. The approach is designed to overcome terrain challenges and prioritize potential wetland areas to ensure a representative sample. Additionally, we avoided areas deemed unsafe by local authorities because of political unrest or crime.

After the first round of sampling for each subregion, we conducted targeted searches for disturbed peatlands within or outside protected areas to ensure a better representation of pasture peatlands. This involved utilizing our preliminary classification maps, aerial drone surveys, and consultations with local guides to identify potential sites. We also collaborated with park rangers and local guides to identify

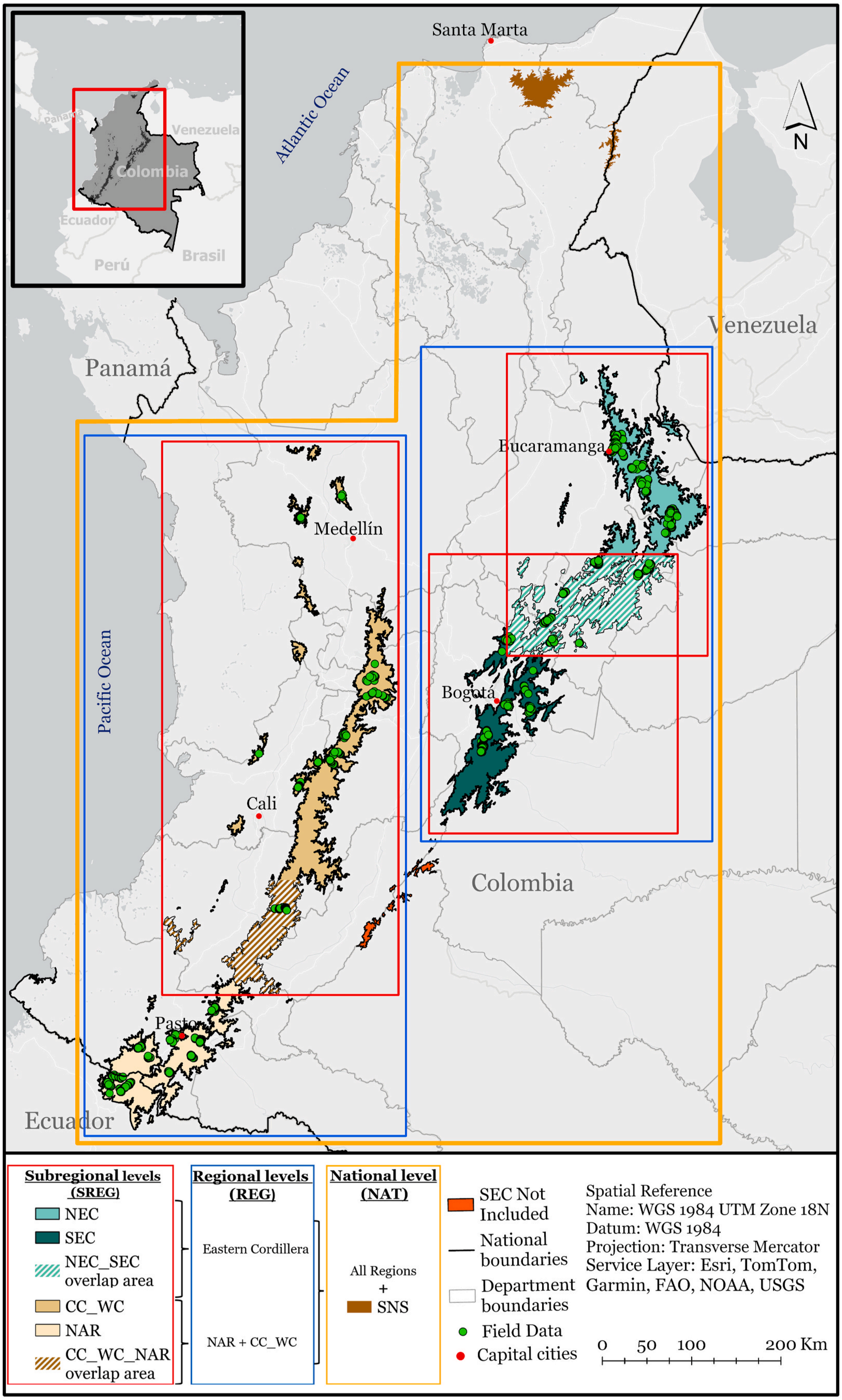

(caption on next page)

Fig. 1. Study area map. Subregional extents (red boxes): Northeastern Cordillera (NEC), Southeastern Cordillera (SEC), Nariño-Putumayo (NAR), and Central and Western Cordilleras (CC_WC). Striped areas show overlaps. Blue colors represent the Eastern Cordillera region; beige colors represent the Nariño and Central/Western Cordilleras region, both surrounded by blue boxes. The Sierra Nevada de Santa Marta and Perijá (SNS) subregion in the north was included in the National extent (Orange box) but had limited analysis due to insufficient field validation data. Green points mark field validation data collection sites.

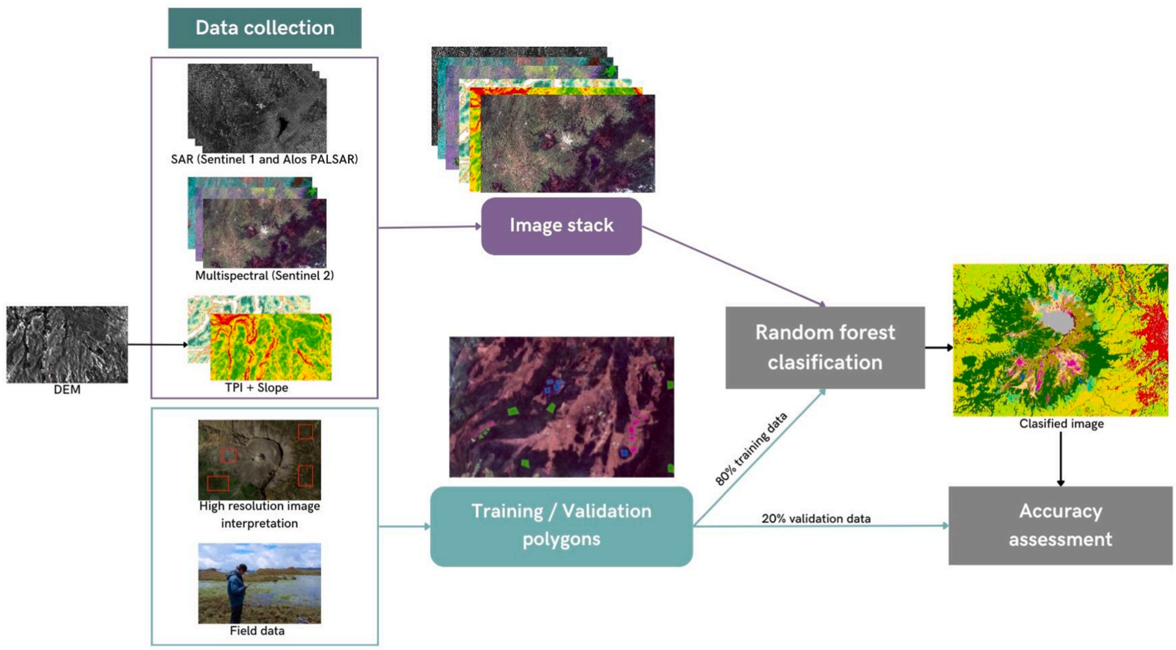

Fig. 2. Peatland mapping methods diagram. Integrated mapping methodology, utilizing field data, multiple remote sensor images, and the Random Forest Algorithm for accurate image classification.

accessible and safe areas that contain a diversity of wetlands and could be covered in a day's work. We still generated random points as described above but permitted minor field adjustments if the original points were unreachable or excessively time consuming to reach, opting for sites with similar apparent LULC classes. For navigation and data collection in the field, we utilized the Avenza Maps mobile application.

At each site, we identified the dominant vegetation and designated a preliminary LULC class. We extracted a 40 cm soil core using a side cutting peat Russian corer, segmented it into 10 cm intervals, and stored them in Zip-lock bags. In peatlands, we recorded additional measurements including peat depth, pH, and specific conductivity. We logged all data into the Epicollect 5 mobile application.

The %C analysis of soils was performed solely to confirm whether the field data points we identified as peatlands actually met the peatland definition (see below). We analyzed the soil samples at The Pontificia Universidad Javeriana's Ecosystems and Climate Change Lab. First, we dried them at 65 °C for 24 h and weighed them to calculate their dry bulk density (BD). We then determined the percentage of organic matter (OM%) and carbon percentage (%C) through loss on ignition at 550 °C for 5 h (Soil Survey Staff, 2014). We calculated the proportion of organic matter using the formula: OM% = ((DW - IW)/DW) x 100, where DW is the oven-dry weight (g) of a subsample before ignition, and IW is the weight (g) after ignition. Assuming the carbon content of dry mass to be 48% of the incinerated organic matter (Loisel et al., 2014), we estimated the carbon percentage as %C = 0.48 × OM%. We determined the BD (g cm^{-3}) by dividing the total dry weight (TW) (g) of each soil sample by the core's volume (cm^3). We determined soil carbon content in Mg per hectare for every 10 cm segment with the equation: Carbon content (Mg ha^{-1}) = BD (g cm^{-3}) × (%C/100) × (10,000 m^2/ha) × Depth (0.1 m).

We validated our field sample classification as peatland vs, non-peatland based on the %C of each soil sample, adhering to the U.S. definition of peatlands. For this study, peatlands are defined as organic soils that are saturated (i.e., waterlogged, with high water content that limits oxygen availability) and contain more than 12% carbon within the first 40 cm of depth. It is essential that the %C in the 30–40 cm layer consistently exceeds 12% (Soil Survey Staff, 2015). When primary or secondary field data sources lacked soil carbon information, we utilized all available resources—including photographs, vegetation composition, saturation levels, and expert consultations—to align each field point with one of our predefined LULC classes, as outlined in Table 1.

2.2.2. Remote sensing data

In our classification strategy, we combined multidate, multi-sensor radar and optical imagery with topographic information from a DEM (Supplementary Material-Table S1), a method proven effective for accurately identifying peatlands in the Andes (Battaglia et al., 2024; Bourgeau-Chavez et al., 2018; Chimner et al., 2019; Hribljan et al., 2017). The approach aims to identify variables such as hydrologic regimes, landforms, soil moisture, and vegetation composition and structure, enabling us to distinguish between peatland types and other wetland or upland classes (Bourgeau-Chavez et al., 2018). We used Sentinel-2 multispectral imagery to provide the classifier with information on vegetation types. However, distinguishing between some upland and wetland LULC classes can be challenging due to their similar spectral signatures. To address this, we integrated SAR imagery from Sentinel-1 and PALSAR, which supplied additional insights into the hydrology and vegetation structure of all LULC classes. Additionally, Topographic Position Index (TPI) and slope data, extracted from the Shuttle Radar Topography Mission (SRTM) DEM, were crucial for distinguishing between flat terrain, valleys, and mountain peaks, playing a key role in the accurate classification of peatlands (Bourgeau-Chavez et al., 2018; Hribljan et al., 2017).

2.2.2.1. Optical imagery – sentinel 2 multispectral imagery. We utilized

Table 1
Land use and land cover (LULC) classes, from lower specificity (Class level 1) to higher specificity with higher levels, including descriptions of these classes.

Class level 1	Class level 2	Class level 3	Class description
Open Water	Open Water	Open Water	Permanently flooded water bodies with no dominant emergent or floating vegetation.
Natural Wetland Areas	Peatlands	Woody/ Shrubby Peatlands	Poorly drained areas with organic soils >40 cm depth and C >12% in Histosols or 25% in Andisols, where woody species dominate (e.g., *Hypericum* spp., *Diplostephium* spp., *Pentacalia* spp.) and or shrubs (e.g., *Chusquea* spp.)
		Herbaceous Peatlands	Poorly drained areas with organic soils (>40 cm depth and C >12% in Histosols or 25% in Andisols), characterized by a matrix dominated by herbaceous species. This includes grasses (e.g., *Calamagrostis* spp., *Agrostis* spp., *Chusquea* spp., *Cortaderia* spp.), sedges (e.g., *Carex* spp., *Richosphera* spp.), rushes (e.g., *Juncus* spp., *Luzula* spp.), ferns (e.g.,*Blechnum* spp.), and herbs (e.g., *Geranium* spp., *Pernettya* spp., *Puya* spp.). While shrubs (e.g. *Diplostephium* spp. *and Hypericum* spp.) may be present, they are not the dominant vegetation.
		Cushion Peatlands	Poorly drained areas with organic soils (>40 cm depth and C >12% in Histosols or 25% in Andisols), dominated by cushion-forming vegetation such as *Distichia muscoides* and *Plantago rigida*.
		Pasture Peatlands	Poorly drained areas with organic soils (>40 cm depth and C >12% in Histosols or 25% in Andisols), characterized by a dominance of naturalized herbaceous species (e.g. *Cenchrus clandestinum, Lolium perenne, Anthoxanthum odoratum, and Trifolium* spp.) These areas may also present native species of grasses, sedges, ferns, and herbs. Typically, these areas exhibit evidence of ditches.
		Sphagnum Peatlands	Poorly drained areas with organic soils (>40 cm depth and C >12% in Histosols or 25% in Andisols), dominated by *Sphagnum* spp. mosses.
	Mineral Wetlands	Wet Meadows	Areas with evidence of saturation and variable water table which contain mineral soils (C <12%) with less than 40 cm in depth, and may be over bedrock. Dominated by herbaceous vegetation and/or mosses.

Table 1 (*continued*)

Class level 1	Class level 2	Class level 3	Class description
		Woody Wetlands	Areas with evidence of saturation and variable water table which contain mineral soils (C <12%) with less than 40 cm in depth. Dominated by woody species like *Escallonia myrtilloides*.
Semi-natural and Natural Upland Areas	Natural Vegetated Upland Areas	Herbaceous Uplands	Areas with non-saturated soils predominantly featuring herbaceous species, including grasses (e.g., *Calamagrostis* spp., *Agrostis* spp., *Festuca* spp.), ferns (e.g., *Jamesonia* spp.), and herbs (e.g., *Geranium* spp., *Pernettya* spp., *Lupinus* spp.). Shrubs such as *Diplostephium* spp. and *Hypericum* spp. may occur but do not dominate the landscape. *Espeletia* spp., when prevalent, are classified within this group.
		Forests	Native Andean and high Andean woody vegetation exceeding 6 m in height (e.g. *Miconia* spp., *Cedrela* spp. *Polylepis* spp. *Quercus* spp.)
		Shrublands	Dominated by native páramo woody vegetation shorter than 6 m (e.g., *Pentacalia* spp., *Hypericum* spp., *Diplostephium* spp., *and Aragoa* spp.)
	Natural Non-Vegetated Surfaces	Bare soil/ rock/sand	Areas with minimal or no vegetation, predominantly characterized by rocks, sand, gravel pits, or quarries. Gravel roads may appear in this category.
		Snow/Glaciers	Areas covered with ice or snow.
Anthropo-genic Land Uses	Productive Areas	Croplands	Agricultural lands where crops are cultivated; in the páramo regions, potatoes and onions are the most common crops.
		Pastures	Lands dedicated to grazing or hay production.
		Forest Plantations	Areas designated for timber production. Homogeneous tree plantings of non-native species such as *Pinus* spp. and *Eucalyptus* spp.
	Urban Areas	Urban Areas	Areas with any man-made infrastructure (e.g. buildings, roads) that is recognizable from satellite images with a spatial resolution of 10m.

Sentinel-2 surface reflectance data, pre-processed for atmospheric corrections, to capture multispectral imagery across the páramo. Sentinel-2's twin satellites provide wide coverage at high resolutions, capturing data in 13 spectral bands to offer detailed insights with a global revisit frequency of five days. This capability is particularly crucial given the challenge of persistent cloud cover in these regions. To address cloud interference, a two-step cloud filtering process was executed through GEE. We initially filtered the images to select those with less than 80% cloud cover. Following this, we applied a cloud probability mask to exclude any pixels with a greater than 10% likelihood of clouds. Finally, we used an edge masking function to remove pixels that might be affected by cloud shadows.

After cloud masking, we included a Normalized Difference Vegetation Index (NDVI) band to help detect vegetation presence and overall productivity, allowing for better differentiation between vegetative land cover classes. The NDVI was calculated from filtered images using the Red and Near-Infrared (NIR) bands with the formula NDVI = (NIR - RED)/(NIR + RED) applied to all filtered and cloud-masked images. This NDVI band was used in combination with ten other spectral bands from Sentinel-2 (e.g., Blue, Green, Red, NIR, SWIR) to create a multi-band composite image. For each pixel, the median value across the selected period was used for the final image composite. This selection was refined through visual assessments to optimize the dataset, particularly in cloud-prone areas, by adjusting the date ranges from 2019 to 2023 for each subregion. There remained an estimated 0.2% residual cloud cover in the final composite, introducing some noise into the classification process for each subregion. We generated a total of 11 layers, shown in Supplementary Material-Table S1.

2.2.2.2. Synthetic Aperture Radar – sentinel 1 (C-band) and ALOS PALSAR (L-band). Synthetic Aperture Radar (SAR) can penetrate clouds, hence offering detailed imagery under all conditions. We utilized SAR imagery from Sentinel-1's C-band and ALOS PALSAR's L-band. The capability of SAR to penetrate vegetation canopies and interact with the ground surface is essential for detecting wetlands, detecting variations in vegetation, structure, and moisture within both the canopy and ground layers.

Given the predominance of short vegetation in páramos, C-band's ability to penetrate a sparse or low-stature vegetation canopy and detect soil moisture offers significant advantages. The Sentinel-1 mission, equipped with a dual-polarization C-band SAR instrument operating at a wavelength of approximately 5.6 cm, corresponding to a frequency of about 5.4 GHz, offers Ground Range Detected (GRD) scenes that are processed to yield calibrated and ortho-corrected products. In Google Earth Engine, the Sentinel-1 data undergoes preprocessing steps including thermal noise removal, radiometric calibration, and terrain correction, to ensure the data accurately reflect surface backscatter while accounting for topographical variations. All available Sentinel-1 images from 2015 to 2022 were converted from decibels to a linear scale, allowing for image compositing by obtaining the mean and standard deviation for all VV and VH polarization during the driest and wettest months. Although the images are not speckle filtered, image compositing effectively serves as temporal multi-looking, thus eliminating the need for additional spatial filtering (Battaglia et al., 2024). Driest and wettest months selection was informed by a decade of precipitation data from IDEAM's meteorological stations, all located above 2750 m, to accurately reflect the climatic conditions of each subregion. As a result, we were able to process 8 layers for our classification analysis, each representing a different season and polarization (Supplementary Material-Table S1).

In parallel to the C-band analysis, we utilized L-band SAR imagery from ALOS PALSAR, operating at a longer wavelength of 24 cm. The longer wavelength is capable of penetrating denser biomass, such as shrubby or woody vegetation found in páramos and sub-páramos, allowing for more effective discrimination of denser vegetation cover types that could also be wetlands. High resolution Radiometrically Terrain Corrected data were downloaded from the NASA Alaska Satellite Facility. We used Fine Beam Dual polarization data, which includes HH and HV polarizations. Given the limited availability of images, we were only able to obtain images between the months of May to October (2006–2011) which mostly correspond to the dry season. To mitigate speckle effects, we applied a 5x5 median filter before temporal averaging, using Python scripts for preprocessing and analysis. Mean, standard deviation, and coefficient of variation were calculated for each polarization over all available images, resulting in a total of 6 layers (Supplementary Material-Table S1).

2.2.2.3. Topographic data – slope and Topographic Position Index. The Shuttle Radar Topography Mission Version 3 product provides a digital elevation model (DEM) at a 1 arc-second (~30 m) resolution, enhanced by void-filling with data from ASTER GDEM2, GMTED2010, and NED for improved global coverage. Our topographic analysis involved calculating the Slope and the TPI from the SRTM DEM using Google Earth Engine. The Slope layer, which indicates the terrain's steepness in degrees, is crucial for identifying potential hydrological dynamics. For the TPI, calculated at neighborhoods of 20 and 50 pixels, approximately 600 m and 1500 m respectively, we evaluated each cell's elevation relative to the average elevation of its surrounding cells. This method assigns positive values to cells that are higher than their average surroundings and negative values to those that are lower, providing a detailed representation of the landscape, helping in identifying potential wetland areas by delineating elevated and depressed terrains. We ultimately obtained three topographic layers from this process.

2.3. Classification approach, accuracy, and congruency assessments

For the classification approach and accuracy assessment, we integrated multispectral and radar data from Sentinel-1, Sentinel-2, and PALSAR, along with topographic data from SRTMGL1. All input datasets, except for SRTM, had an original spatial resolution of 10 m. To ensure consistency across layers, SRTM data was resampled to 10 m using nearest-neighbor interpolation. These datasets were combined into a unified image stack at a 10 m spatial resolution, serving as the input for the Random Forest (RF) classification. All input variables were included, as previous research in peatland mapping has shown that variable importance rankings for the entire model may not reflect their significance for individual classes, making it essential to retain variables that may be critical predictors for specific classes (Bourgeau-Chavez et al., 2021). The classification was performed at Level 3 of the LULC hierarchy, as described in Table 1. Before running any classification, we calculated mean pixel values within our training and validation polygons of all the 28 layers of the image stack, carefully excluding outliers to minimize classification noise. Excluded outliers predominantly consisted of polygons that were drawn over areas affected by optical imagery disturbances, such as clouds, shadows, and fog.

To train the classifier, we used polygons representing approximately 80% of the total training polygon area for each class, reserving the remaining 20% for validation purposes. Field visited polygons were prioritized for validation. The division into training and validation sets was conducted randomly for each subregion. For comparability among maps, we retained the same validation and training polygons for both Regional and National spatial extent classifications. For these classifications, we merged the training and validation polygons of subregions within the same region, and subsequently combined all for the National spatial extent classification.

The RF algorithm implemented in R, selected for its proven effectiveness in wetland mapping (Battaglia et al., 2024; Bourgeau-Chavez et al., 2017, 2018; Chimner et al., 2019; Hribljan et al., 2017), processes the data through a series of decision trees based on random data subsets and training layers, with the final classification based on majority voting among the trees (Breiman, 2001). The model was configured with 500 decision trees, and the variable selection for each node split was set to the default value, corresponding to the square root of the total input variables. This approach, as detailed by Battaglia et al. (2024), adheres to widely accepted practices in land cover classification using the Random Forest algorithm. Such parameter choices have consistently delivered reliable results in prior studies involving multi-source remote sensing data (Belgiu and Drăguţ, 2016; Forkuor et al., 2014; Mahdianpari et al., 2020; Spagnuolo et al., 2020). The model's performance was evaluated using producer's and user's accuracy metrics, calculated based on the reserved validation polygons, following the established procedures outlined by Congalton and Green (2019).

Following the classification with the RF algorithm, we employed

ESRI's 'Mosaic to New Raster' tool to combine corresponding classified subregions and regions sections into the SREG and REG maps respectively. Where overlaps between NEC-SEC and CC_WC-NAR occur, we prioritized classifications from NEC and NAR for their higher accuracy. Three national maps were then our final product: SREG, REG and NAT. The NAT map covers a larger area as it includes the SNS subregion, for which no field validation data were collected. To aid classification in the SNS, we used training data from the rest of the country. We masked out the SNS subregion when comparing with the other maps to ensure consistent areas. While we report pixel-based areas for the SNS, further accuracy analysis will require field validation data, so should be considered preliminary findings only.

We post-processed these three classification maps to reduce errors and improve their quality and accuracy. Using the ESRI's majority filter, we refined our maps by adjusting each pixel's value to reflect the majority class among its eight neighbors, which improved accuracy but occasionally removed smaller features. To address misclassifications caused by noise in Sentinel-2 imagery, such as clouds, shadows, and spectral distortions, we made several targeted corrections: For areas classified as cushion peatlands below 3700 masl, we reclassified them by assigning values based on the majority within a 10x10 cell neighborhood. Although it is known that cushion peatlands in the country are typically found above 4000 masl (Benavides et al., 2023), we selected the 3700 masl limit due to field findings of dominant *Plantago* spp. peatlands around this elevation. We follow a similar approach for misclassified Glacier/snow pixels due to cloud pixels, replacing all glacier/snow pixels below 4500 (no glaciers found below this elevation in Colombia), and reassigning values based on the majority within a 20x20 cell neighborhood. Bare rock and urban areas are sometimes misclassified due to spectral similarities rock has with cement. Given the unlikelihood of significant human settlements over 4000 masl and the abundant bare rocks in periglacial zones, we corrected misclassifications as urban areas at these elevations by reclassifying them to the bare rock class. Additionally, using the OpenStreetMap Road layer for Colombia, we buffered main roads by 3 m and rasterized this to 10-m pixels, replacing these pixels into the map.

2.4. Estimating peatland areas and distribution

2.4.1. Peatland area estimation

To estimate the total area of peatlands, we used a pixel-based approach applied to our classified land cover maps. The number of pixels assigned to each class was counted and multiplied by the area of a single pixel. Given a spatial resolution of 10 m, each pixel covered 100 m^2. The total pixel count for each class was then multiplied by 100 and converted to hectares by dividing by 10,000.

However, due to errors of omission and commission, the mapped peatland area may differ from the actual extent (Hribljan et al., 2017). To adjust for classification inaccuracies, we applied an area estimation approach using the error matrix and the proportional area of each class (Olofsson et al., 2013). This approach assumes a random, systematic, or stratified random sample of field validation points. Our field validation samples were collected through extensive field visits, primarily from our main field sites, using a stratified random sampling method. Additionally, targeted sampling was employed to ensure a comprehensive representation of various peatland types and conditions.

2.4.2. Peatland distribution by size and elevation

To analyze peatland distribution across size classes and elevation ranges, we extracted peatland classes from the classified raster maps and converted them into polygons. The area of each peatland polygon was calculated and categorized into predefined size classes.

To assess elevation, we determined the centroid of each peatland polygon and extracted its elevation value from a Digital Elevation Model (DEM). While we acknowledge that larger peatlands may span a range of elevations, we assumed that the centroid provides a reasonable approximation, as peatlands are generally associated with flat terrain. The extracted elevation values were then categorized into predefined elevation bands.

2.4.3. Peatland congruency assessment

We conducted a peatland congruency analysis to better understand the differences among our three final maps. We began by reclassifying peatland types into a single peatland class. The reclassification allowed us to compare the three maps to assess overlaps in peatland areas. Using this method, we could easily identify areas of congruence or divergence among maps. Following reclassification, we separated areas where peatland classification coincided in all three maps. We generated three buffer areas of 1, 3, and 5 cells, which we used as masks to extract peatland classifications from our original congruency map that fell within these buffered zones. The analysis helps us quantify if peatland areas classified by only one or two maps are adjacent or non-adjacent to peatland areas where all three maps coincide.

2.5. Evaluating peatland degradation across protected areas and páramo complexes

We used the official Protected Areas layer from National Parks of Colombia (Sarmiento Pinzón et al., 2013) to extract only the regions within protected areas from our three classified maps (SREG, REG, and NAT) and estimated the area of each land cover class using a pixel count method. To evaluate land cover distribution within páramo complexes, we utilized the Tabulate Area tool in ArcGIS Pro to calculate the total area of each land cover class within these complexes in Colombia. We automated processing with a Python script using arcpy, batch-processing our three maps and converting pixel counts to hectares. Páramo complexes were used as analysis units as they represent the proposed official delimitation by the Colombian Ministry of Environment for conservation planning (Sarmiento Pinzón et al., 2013). While still in the process of being formalized, these limits are widely used in research (Galvis et al., 2021). Some páramo complexes extend beyond our study area, but the excluded regions consist mainly of Andean forests, meaning that the representation of peatlands within the páramo complexes remains largely intact. This analysis assessed peatland distribution within individual páramo complexes and human disturbances, particularly in pasture peatlands. We calculated their proportion relative to both the total páramo complex area and the total peatland area to evaluate peatland degradation within each páramo complex. We examined 32 of 37 páramo complexes in this analysis, excluding Perijá and Sierra Nevada de Santa Marta due to field data limitations on the mapped area, as well as Picachos and Miraflores in the southern section of the Eastern Cordillera, which was excluded due to insufficient field data and persistent cloud cover in satellite imagery (Fig. 1). The Las Baldías complex was also omitted due to its small size and mainly forest cover.

3. Results

3.1. National mountain peatland maps of Colombia

We mapped 17 LULC classes, including five peatland-specific classes— one of which identifies disturbed peatlands (pasture peatlands). Other classes include an open water class, two mineral wetland types, five semi-natural and natural upland areas, and four anthropogenic land use classes.

Pooled peatland producer's, peatland user's, and overall accuracies were consistently high across all three maps (SREG, REG, NAT), with values between 92 and 94%, 87–88%, and 90–93%, respectively (Table 2). Notably, the wet meadow and woody wetlands classes exhibited lower accuracy, with producer's accuracy for wet meadows at 43–57% and user's accuracy at 43–50%. Woody Wetlands' producer's accuracy varied between 17 and 54% and user's accuracy between 12

Table 2
Summarizes the producer's accuracy (PA) and user's accuracy (UA) for LULC classes across the three national maps: subregional (SREG), regional (REG), and national (NAT).

Class	SREG		REG		NAT	
	PA	UA	PA	UA	PA	UA
Open Water	100%	100%	100%	100%	100%	100%
Woody/Shrubby Peatlands	83%	73%	68%	62%	66%	58%
Herbaceous Peatlands	86%	75%	79%	75%	78%	74%
Cushion Peatlands	89%	98%	92%	99%	90%	100%
Wet Meadows	54%	48%	48%	43%	57%	50%
Pasture Peatlands	93%	86%	91%	83%	89%	80%
Sphagnum Peatlands	87%	94%	86%	89%	85%	90%
Woody Wetlands	54%	38%	17%	12%	26%	30%
Forests	92%	97%	90%	97%	89%	97%
Herbaceous Uplands	88%	87%	88%	78%	89%	74%
Bare soil/rock/sand	98%	99%	95%	99%	96%	98%
Shrublands	72%	71%	64%	64%	59%	60%
Snow/glaciers	100%	100%	100%	100%	100%	100%
Pastures	93%	98%	86%	96%	83%	93%
Croplands	95%	73%	90%	66%	86%	65%
Forest plantations	75%	81%	81%	90%	79%	85%
Urban areas	95%	96%	96%	89%	95%	92%
Overall Peatland's Accuracy	**94%**	**87%**	**92%**	**88%**	**92%**	**88%**
Overall Accuracy	**93%**		**90%**		**90%**	

and 38%. Although some peatland type producer's and user's accuracies appear to be low, they mostly are confused with other peatland classes, hence the high overall peatland producer's and user's accuracies (see confusion matrices in Supplementary Material-Tables S2-S4).

3.2. Peatland area and distribution

The peatland areas (based on pixel counting) for the entire study area on these maps measured 221,825 ha (SREG), 215,023 ha (REG), and 187,280 ha (NAT), accounting for 4.8%, 4.7%, and 4.1% of the total mapped area, respectively (Supplementary Material-Table S5). Total areas for all classes within the Colombia national border are presented in Table 3, with adjusted areas consistently higher than the mapped areas. The results are presented as ranges representing the minimum and maximum values among our three maps. Herbaceous and woody/ shrubby peatlands proved to be the most extensive peatland classes, representing 40–43% and 39–43% of all peatlands, respectively. Pasture peatland areas ranged from 13 to 15% of the total peatland area. *Sphagnum* peatlands covered 2–3% of all peatland area. Cushion peatlands represented the least extensive peatland class, representing 1% of the total peatland area for all three maps.

The peatland extent varied significantly with elevation (Fig. 3). All peatland classes, except for cushions, are found between 2750 and 4500 m, with most peatlands occurring between 3250 and 3750 m (62%). Herbaceous and woody/shrubby peatlands are present at all elevations, but herbaceous peatlands are more abundant above 3500 m, while woody/shrubby peatlands dominate below 3500 m. Cushion peatlands were found above 3700 m, with *Plantago rigida* being the most dominant below 4000 m and *Distichia muscoides* above 4000 m. Overall, cushion peatlands are more abundant between 4000 and 4500 m. Conversely, *Sphagnum* peatlands are more abundant at lower elevations (2750–3000 m) and gradually decrease as elevation increases.

The combined peatland areas, i.e., locations mapped as peatlands in at least one of the three maps, totaled 294,165 ha. Of these, 132,098 ha (45%) were consistently classified as peatland by all maps. When examining the areas adjacent to this 45% congruent region, we observed distinct patterns. Specifically, 21%, 36%, and 42% of the peatland areas classified by only one or two maps were located near the regions where all three maps overlapped, within distances of 1, 3, and 5 cells (each cell representing 10 m), respectively. This suggest that the discrepancies between the maps are predominantly at the edges of the peatlands, indicating a high likelihood of agreement in peatland location. In other words, 42% of the total peatland areas in the three maps are within 50 m of the regions where all maps are congruent. Many of these zones are likely gradual ecotones where transition to shallower peat makes distinguishing peat from other classes difficult. The remaining 13% of discrepancies can be attributed to isolated pixels classified by each map and the larger areas of pasture peatlands in the NEC subregion identified only in the SREG map as shown in Fig. 4.

3.3. Degraded peatlands

Across all three maps, 13–15% of the total peatland area has been converted into pasture peatlands. While 51% of mapped peatlands fall within protected areas designated by the National System of Protected Areas (SINAP), 7–8% of these peatlands have still been converted into pasture (Supplementary Material-Table S6). This degradation varies across different páramo complexes, with some areas experiencing particularly high levels of pasture conversion. Complexes with more than 30% of their total peatlands classified as pasture peatlands in at least one of the maps include Almorzadero (44–63%), Jurisdicciones-Santurbán-Berlín (36–45%), Sierra Nevada del Cocuy (31–40%), and Tota - Bijagual - Mamapacha (9–34%), all situated within the NEC subregion (Fig. 1). Additionally, several complexes exhibit moderate degradation, with pasture peatlands making up more than 15% of total peatlands in at least one of the maps. These include Chiles Cumbal (15–18%), Los Nevados (10–26%), Guantiva - La Rusia (17–23%), Pisba (12–29%), Sonsón (10–16%), and Altiplano Cundiboyacense (10–17%).

Complexes with relatively high peatland area and low peatland disturbance include Cruz Verde - Sumapaz, the largest páramo complex with the most extensive peatland area, with 26,559–32,449 ha of peatlands and 2–3% classified as pasture peatlands. Las Hermosas follows with a total peatland area between 8134–14,361 ha, with 2–8% converted to pasture. La Cocha-Patascoy contains 8152–11,038 ha of peatlands, with pasture peatlands accounting for just 1–2%. Nevado del Huila and Chingaza have among the lowest levels of disturbance, with peatland degradation between 0.6-3% and 0.9–1.1%, respectively. Table S7 in Supplementary Material summarizing all páramo complexes, their total peatland areas, and the percentage of pasture peatlands relative to total peatlands is provided in the supplementary material.

3.4. Soil carbon analysis (0–40 cm of depth)

Clear differences in carbon percentage (%C) and bulk density (g/ cm^3) at depths of 0–40 cm are evident across various land cover types (Fig. 5). Herbaceous and *Sphagnum* peatlands are combined due to limited primary field data for *Sphagnum* peatlands. This combination is logical as *Sphagnum* peatlands are typically integrated within herbaceous peatlands. For all classes, %C generally decreases with depth, with non-peatland classes showing a more abrupt decline. Peatlands consistently exhibit the highest %C at all depths (e.g., Cushion peatlands: 33% at 0–10 cm to 29.5% at 30–40 cm; Herbaceous peatlands: 30.5% at 0–10 cm to 25.1% at 30–40 cm). Additionally, peatlands have low bulk densities that increase slightly with depth (e.g., Cushion peatlands: 0.09 g/cm^3 at 0–10 cm to 0.14 g/cm^3 at 30–40 cm; Herbaceous peatlands: 0.11 g/cm^3 at 0–10 cm to 0.19 g/cm^3 at 30–40 cm). However, within the peatland categories pasture peatlands exhibit lower %C and higher bulk density likely because drainage leads to subsidence and exposes peat to oxygen, facilitating microbial decomposition of organic matter. As the water table drops in drained peatlands, the peat structure becomes more compact, leading to higher bulk density. The oxidation reduces the carbon storage of these peatlands, highlighting the detrimental effects of land-use changes on peatland ecosystems. Additionally, soil compaction from livestock further increases bulk density, reducing the soil's ability to retain water and exacerbating degradation.

Table 3
Mapped areas within Colombia national borders (based on pixel counting) and adjusted areas (using a stratified estimator) with its respective margin error (95% CI) of LULC classes. Small differences in the total area of the maps are due to pixel variation at the edges, primarily resulting from resampling pixels (nearest neighbor) when generating the mosaics. We included the areas estimated in the Sierra Nevada de Santa Marta (SNS); however, we did not calculate the adjusted area because we did not have any g field validation in this region of the country.

LULC Classes	SREG				REG				NAT				SNS	
	Area (ha)	Area %	Adjusted Area (ha)	Adjusted Area (%)	Area (ha)	Area %	Adjusted Area (ha)	Adjusted Area (%)	Area (ha)	Area %	Adjusted Area (ha)	Adjusted Area (%)	Area (ha)	Area %
Open Water	19134	0.44%	19337 ± 254	0.44%	19230	0.44%	19823 ± 936	0.45%	18989	0.44%	19216 ± 260	0.44%	1708	0.92%
Woody/Shrubby Peatlands	90932	2.08%	99134 ± 7685	2.27%	83877	1.92%	84955 ± 6451	1.95%	79939	1.83%	76952 ± 6547	1.76%	82	0.04%
Herbaceous Peatlands	78491	1.80%	89661 ± 4191	2.05%	85382	1.96%	116800 ± 6615	2.67%	68430	1.57%	103432 ± 5955	2.37%	391	0.21%
Cushion Peatlands	2802	0.06%	5804 ± 1007	0.13%	2623	0.06%	5981 ± 1177	0.14%	2096	0.05%	6080 ± 1568	0.14%	3	0.00%
Wet Meadows	9596	0.22%	9219 ± 1531	0.21%	16486	0.38%	16336 ± 2421	0.37%	12058	0.28%	11215 ± 1663	0.26%	208	0.11%
Pasture Peatlands	30853	0.71%	33080 ± 2232	0.76%	27669	0.63%	33858 ± 2908	0.78%	22520	0.52%	29380 ± 2940	0.67%	99	0.05%
Sphagnum Peatlands	6364	0.15%	9585 ± 1142	0.22%	3898	0.09%	8712 ± 1950	0.20%	4200	0.10%	9005 ± 2233	0.21%	1	0.00%
Woody Wetlands	10662	0.24%	4663 ± 1479	0.11%	13761	0.32%	5168 ± 2334	0.12%	7759	0.18%	4670 ± 2206	0.11%	39	0.02%
Forests	1636449	37.47%	1804309 ± 15412	41.31%	1730408	39.63%	1960164 ± 16885	44.89%	1644405	37.68%	1878286 ± 16859	43.03%	20573	11.12%
Herbaceous Uplands	629659	14.42%	645747 ± 13472	14.79%	639773	14.65%	599672 ± 13842	13.73%	758606	17.38%	690871 ± 16664	15.83%	47493	25.68%
Bare soil/rock/sand	97886	2.24%	115962 ± 3244	2.66%	91863	2.10%	107222 ± 2781	2.46%	95629	2.19%	113020 ± 3131	2.59%	84102	45.47%
Shrublands	847267	19.40%	652175 ± 19410	14.93%	749780	17.17%	547567 ± 18520	12.54%	808723	18.53%	563173 ± 20468	12.90%	26634	14.40%
Snow/glaciers	2964	0.07%	2964 ± 0	0.07%	2967	0.07%	2967 ± 0	0.07%	3068	0.07%	3068 ± 0	0.07%	889	0.48%
Croplands	115516	2.64%	204690 ± 8881	4.69%	143284	3.28%	288294 ± 9925	6.60%	145391	3.33%	317810 ± 11839	7.28%	229	0.12%
Pastures	766519	17.55%	566768 ± 10994	12.98%	732419	16.77%	498178 ± 10808	11.41%	664583	15.23%	444997 ± 9775	10.20%	2356	1.27%
Forest Plantations	12305	0.28%	90781 ± 10217	2.08%	12215	0.28%	57149 ± 6359	1.31%	18035	0.41%	79812 ± 8911	1.83%	125	0.07%
Urban Areas	10124	0.23%	13643 ± 1762	0.31%	11209	0.26%	13998 ± 1823	0.32%	10277	0.24%	13720 ± 1704	0.31%	19	0.01%
Total Peatlands	**209442**		**237264 ± 16258**		**203449**		**250306 ± 19100**		**177185**		**224848 ± 19244**		**576**	
Percentage of Peatlands		**4.80%**	**5.43%**			**4.66%**	**5.73%**			**4.06%**	**5.15%**			**0.31%**
Total Area	**4367522**				**4366844**				**4364707**				**184951**	

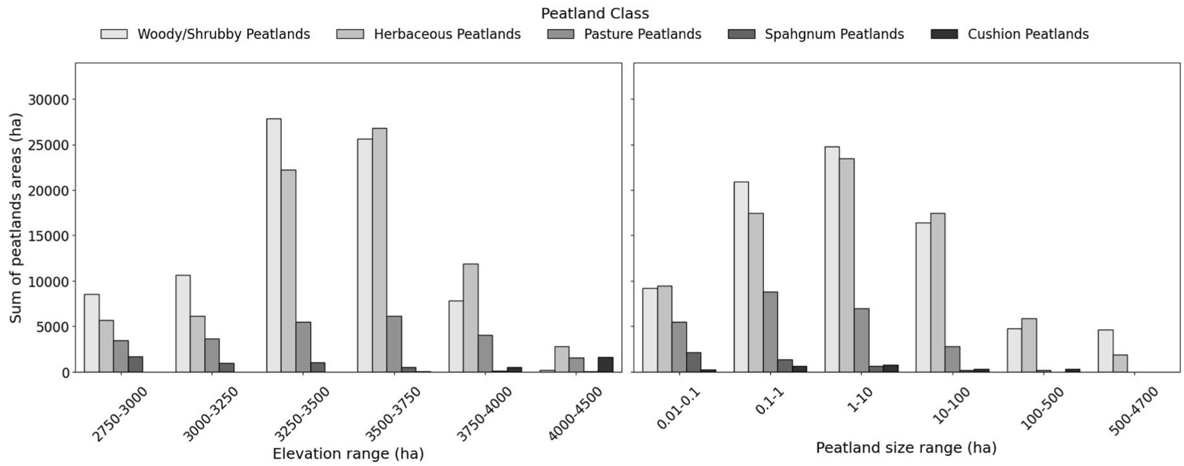

Fig. 3. Distribution of peatland areas by elevation (left) and peatland size range (right) for the NAT map. Patterns are consistent across the three national maps (SREG, REG, NAT), with minor variations in total peatland area. Bars represent the sum of peatland areas (ha) by class: Woody/Shrubby, Herbaceous, Pasture, Sphagnum, and Cushion Peatlands.

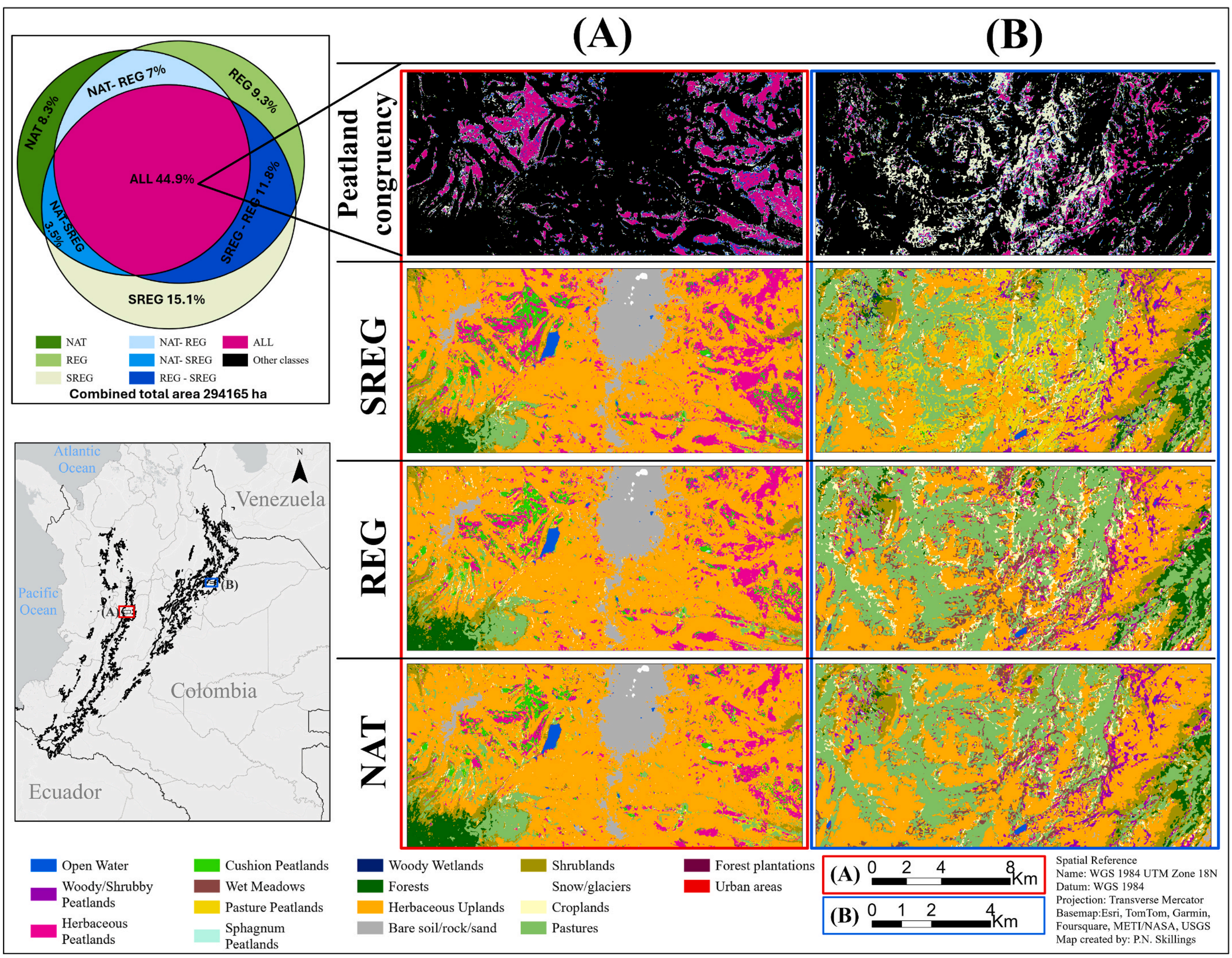

Fig. 4. Comparison of peatland distribution across three classification maps: SREG, REG, and NAT. Maps in column (A) show an area in Nevados National Park, highlighting typical significant peatland congruency, with SREG regions appearing larger than NAT regions upon close inspection. Site (B), located in the department of Boyacá, demonstrates discrepancies in peatland classification: the SREG map shows a large area of pasture peatlands, while the REG and NAT maps classify the same area as either pastures, croplands or wet meadows. The maps at the top of both columns show the combined peatland area for the three maps, with a Venn diagram on the left illustrating the total area percentages of congruence between the three maps.

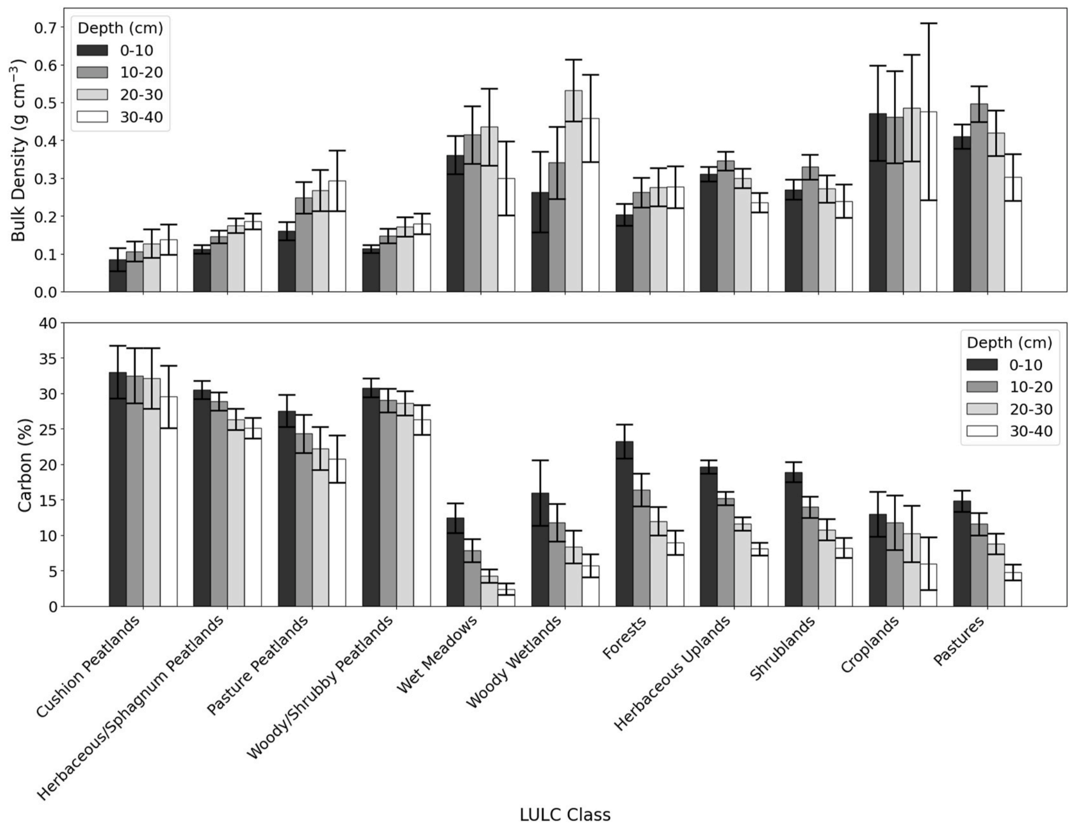

Fig. 5. Averaged bulk density and averaged carbon percentage across different LULC classes at various soil depths. Error bars represent 95% confidence intervals.

4. Discussion

4.1. National peatland maps of Colombia

Advantages and disadvantages of each of the three maps created using different spatial extents were observed. Smaller spatial extent classifications benefit from similar environmental conditions and vegetation composition. In a smaller footprint we expect more uniformity within these localized areas, which reduces variability in the data. Additionally, the overall computing time for classification is faster than processing larger regions of our study area. However, in the case of the SREG level approach, merging adjacent subregions into a cohesive map is challenging, as differences from independent classifications are much more notable at adjacent borders of these subregions. Furthermore, limited training and validation data in smaller extents may fail to represent some classes, especially those hard to find in the field or interpret with high-resolution techniques. Conversely, larger spatial extents cover broader areas, leveraging a more extensive range of training data to address gaps but potentially lacking the detail needed for capturing local variations and requiring more computational time.

Discrepancies across the three maps are mainly found at the peatland edges, especially in shallow peat zones or transitional areas between peatlands and other ecosystems. These edge effects likely result from gradual ecotones, where environmental and vegetation characteristics shift gradually rather than abruptly. This has implications for both peatland mapping and carbon stock estimation, as edge areas may have different carbon accumulation dynamics and depths compared to central areas of peatlands. Mapping inconsistencies at the edges could lead to under- or overestimation of peatland extents, affecting total carbon stock calculations. Future studies should aim to refine classification techniques in these transitional areas by incorporating additional field data and utilizing probabilistic classification methods that account for uncertainty in ecotonal boundaries.

For peatland assessment in the field, we recommend using the combined peatland area from the three maps since there is a better chance of finding peatlands where all three maps are congruent without discarding areas that might contain shallow peatland areas or that were not classified in one or two of the maps. By comparing the three maps, we can better plan further field validation to improve future versions of the national peatland map.

Importantly, the SREG and REG maps will not represent all LULC classes due to the lack of field data for some classes in certain subregions. In contrast, the NAT map included classified areas for all LULC classes across all subregions because it combined training data from all subregions. Ideally, each subregion should have significant amounts of training data for each class, but field validation is often difficult to achieve because of limited extent of individual classes, access constraints, and the expense of fieldwork. This limitation was particularly evident for wet meadows and woody wetlands, which had the least amount of traing data (Fig. S1) and were often confused with peatland classes (Supplementary Material-Tables S2-S4). Improving field data coverage in underrepresented areas would help refine the classification of these ecosystems and reduce misclassification with peatlands.

4.1.1. Comparisons with existing maps

4.1.1.1. Global peatland map 2.0. High-resolution mapping is crucial for informing global peatland maps, which often rely on compiled datasets and lack detailed data for specific regions, such as on mountain peatlands in the tropics (Gumbricht et al., 2017; Melton et al., 2022; UNEP, 2022; Xu et al., 2018). The GPM2, for example, was produced by compiling existing maps, many of which did not include accurate or high-resolution data for páramo peatlands in Colombia. As a result, GPM2 estimated a much lower ~37,500 ha of peatlands within our study area (Greifswald Mire Centre, 2022), of which only 27% align with our mapped peatland areas. The discrepancy is primarily due to the significantly lower spatial resolution (1 km^2 pixels) of the GPM2 map vs. our 100 m^2 pixels (Fig. 7), reducing their ability to detect smaller peatlands. Although the GPM2 estimates that only 1% of all peatlands in the country occur above 2750 m, our study suggests that 5–6% of the country's peatlands are found above this elevation. Additionally, 75–80% of the total area of mapped peatlands had individual sizes under 100 ha, highlighting the importance of high-resolution mapping for accurately identifying mountain peatlands (Fig. 3).

4.1.1.2. National maps of Colombia. The 2015 National Wetland Map of Colombia (NWMC) combines geomorphological, soil, land cover, hydrographic, and flood frequency data to identify wetlands at a 25-m spatial resolution (Flórez-Ayala et al., 2016; Jaramillo Villa et al., 2016). It categorizes wetlands based on water presence and environmental traits into the following classes: Permanent Open, with visible and continuous water; Permanent Under Canopy, where water is ever-present beneath forest cover; Temporal, with fluctuating water levels; and Medium and Low Potential, suggesting probable but uncertain wetland conditions. Comparing the combined peatland areas from our maps with this map, we found that only 34.7% of the peatland area falls within its wetland classes, mainly as Low Potential wetlands (32.1%) and Temporary Wetlands (2.6%). Additionally, the National Wetland Map classifies about 850,000 ha of wetlands in our study area, including open water and glaciers as Permanent Open wetlands (Fig. 7). In contrast, we estimated (using adjusted areas) 240,734–271,810 ha of combined mineral wetlands and peatlands, with combined areas of open water and glacier/snow classes accounting for 22,284–22,790 ha. While the NWMC provides a broad estimate of wetland areas, its general classifications do not capture the specific types and extents of wetlands needed for detailed ecological studies and management of peatlands (Fig. 7). The broad categories and the integration of various mapping products, with differences in resolution and classification criteria, may introduce errors and overestimate wetland areas.

In contrast, the 2018 National Land Cover Map of Colombia (NLCMC), developed at a 1:100,000 scale using the Corine Land Cover methodology, employs Landsat satellite images for visual interpretation and reports a 91% overall accuracy across 54 land cover classes, including a peatland class (Castellanos et al., 2021). The classification was performed using the Photo-Interprétation Assistée par Ordinateur technique, which involves visual interpretation of satellite images on a screen. Although it claims 100% user's and producer's accuracies for the peatland class, the map only reports 11 peatland polygons totaling 793.3 ha within our study area. Comparing our map to this official land cover map, we found that 70% of peatlands in the NLCMC are classified as Herbaceous uplands, 16% as Pastures, 10% as Shrublands, and 3% as Forests, with the remaining 1% in other classes.

Although the NLCMC map is widely used, it lacks thorough wetland data, mainly because Landsat imagery alone is insufficient for mapping wetlands and because of inadequate field validation to resolve peatland classes. The accuracy assessment for the NLCMC involved assigning reference labels to sampling points based on visual interpretation, without extensive field validation specifically for peatlands. In contrast, peatland mapping studies have shown improved results using a multi-date, multi-sensor SAR and optical approach, combined with extensive field data (Bourgeau-Chavez et al., 2018). For example, Hribljan et al. (2017) compared classification accuracies using several remote sensor data for mapping alpine peatlands in northern Ecuador. Using Landsat-only optical imagery, they achieved an overall accuracy of 86% but had moderate errors in distinguishing between peatland classes. When combined with Radarsat, PALSAR, and TPI data, the overall accuracy increased to 90%, with most individual peatland class accuracies also improving or remaining the same. The comparison underscores the limitations of the NLCMC in accurately representing peatland areas. Relying solely on visual image interpretation and Landsat imagery without extensive field validation data leads to inaccuracies, especially for mapping wetlands.

4.1.1.3. Regional maps from the andes. When comparing our findings with other studies in the Andes, notable differences emerge regarding proportions of peatland area with total mapped area. The Ecuadorian Andes páramo peatland map estimates peatland coverage at 18% of the total mapped area of 271,492 ha above 3500 m (Hribljan et al., 2017). Similarly, in Peru, the Huascaran National Park and its buffer areas in the puna region, covering a total area of 510,200 ha, estimate peatlands to cover approximately 6.3%, primarily consisting of cushion peatlands at elevations between 3950 and 4650 m (Chimner et al., 2019). In Colombia, regional peatland maps for the Las Hermosas, Chili-Barragán, and Guanacas-Purace-Coconucos páramo complexes reported peatland coverage of 40,337 ha, representing 9.4% of the total mapped area of 429,530 ha (Battaglia et al., 2024).

Although our study shows that within the entire study area peatlands only cover 4.0–4.8%, we used a lower elevation boundary of 2750 m compared to other mapping efforts. The lower boundary allowed us to detect peatlands in azonal páramos (páramos that occur in areas influenced by specific local conditions rather than the typical high-altitude environments) and in transformed areas where peatlands might still exist. Our approach includes large proportions of areas of Andean forests, pastures, and croplands that are not considered in other maps. When estimating the total peatland area from an elevation greater than 3500 m (Supplementary Material-Table S8), the peatland percentage increased to 7.7–10.2% of the total area. Moreover, pasture peatlands over 3500 m accounted for 14–17% of all peatland categories.

4.1.2. Peatland mapping challenges

Mapping peatlands in the Andes presents several challenges. First, constant cloud cover in these mountainous ecosystems makes the acquisition of cloud-free optical images from Sentinel-2 difficult. Although we used Google Earth Engine (GEE) to automate the selection of the best pixels possible through cloud masking techniques, we still encountered several defects in our images, especially in cloud forests and steep valleys. Shadows, fog, and clouds introduced noise, affecting classification results. Visual inspections of the map suggest that many areas where we detected noise in the optical imagery have misclassified forests or shrublands as pastures and some herbaceous uplands as croplands. While our focus in these maps is on peatlands, and we consider these classes to be accurate, there may be some errors in upland classification classes due to these defects in the optical images.

Regarding SAR imagery, emerging technologies will likely improve classification results for dense vegetation classes. Our woody wetlands and shrublands classes, which currently show lower accuracy, might achieve better results with upcoming available high-resolution SAR data. The NASA/ISRO NISAR sensor, expected to provide global L-band SAR coverage with a twelve-day repeat cycle, and the recently launched ALOS-4/PALSAR-3 satellite (July 2024) will offer more frequent and detailed observations. These sensors, along with the continuity of data from ALOS-2/PALSAR-2, will deliver consistent and higher-resolution datasets, offering new opportunities for enhancing the accuracy of land cover classifications. Specifically, they will improve our ability to distinguish dense vegetation types and further refine peatland mapping efforts in the Andes, where vegetation density and terrain complexity have historically posed challenges for remote sensing approaches.

4.2. Degraded mountain peatlands

This study reveals that 13–15% of all peatland areas have been converted into pasture peatlands. This transformation has significant implications for greenhouse gas emissions and water supply. Even though 51% of the peatlands identified across all three maps fall within protected areas under the National System of Protected Areas (SINAP), disturbances were frequently observed during field visits (Fig. 6).

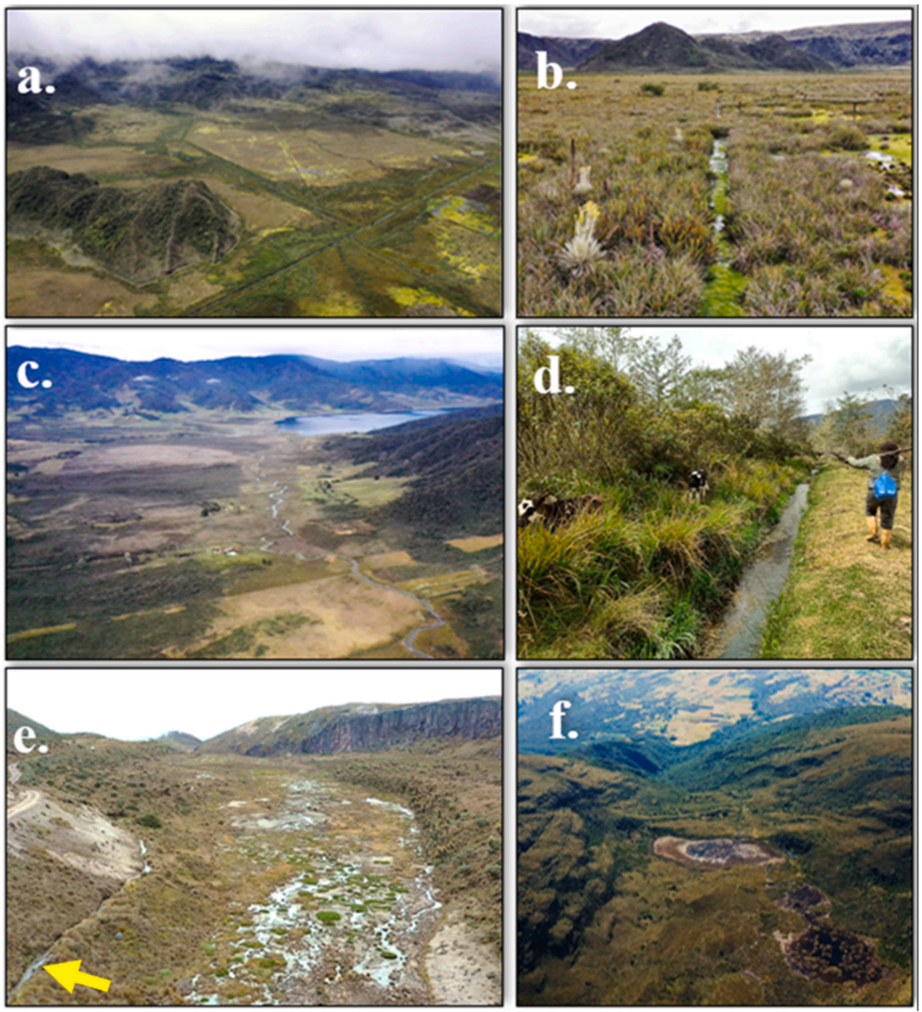

Fig. 6. Disturbed peatland landscapes. (a) and (b) show the Vista Hermosa de Monquentiva Regional Park in Cundinamarca. (a) An aerial image of a peatland complex (Sphagnum, herbaceous, and shrubby peatlands) with unsuccessful drainage ditches. (b) A closer view of a small ditch within the peatland complex. (c) and (d) show the Protected Forest Reserve in Laguna La Cocha and Cerro Patascoy. (c) An aerial image of a disturbed section of the largest peatland complex in Colombia. (d) A close-up of peatland areas affected by drainage efforts. (e) Shows the Alfombrales area in Los Nevados National Park, where a ditch (pointed with the yellow arrow) diverts glacial water, causing severe damage to cushion peatlands. (f) Displays the "Ojo de Agua" peatland in Iguaque National Park, where water is extracted for agriculture using buried hoses.

Notably, 7–8% of the peatlands within these protected areas are classified as pasture peatlands, underscoring the urgent need for integrated management strategies that prioritize peatland conservation (Supplementary Material - Table S6). The persistence of degradation within protected areas suggests that current conservation efforts may be insufficient, likely due to limited awareness among land managers, decision-makers, and the public regarding the critical ecosystem services peatlands provide, such as hydrologic regulation and carbon storage, as well as their susceptibility to degradation, which can lead to long-term ecological damage.

A broader spatial assessment of Colombia's human footprint confirms that the Andean region, including páramos, is among the most impacted areas due to increasing human activity over the past four decades (Correa et al., 2020). Agricultural expansion, infrastructure development, and intensified land use have driven substantial transformations in the highlands. These pressures are particularly evident in pasture peatlands, which are predominantly concentrated in the northern part of the Eastern Cordillera, as well as in the Central Cordillera, particularly within the Los Nevados páramo complex, and in the southern Andes in the Nariño-Putumayo subregion, specifically in the Chiles-Cumbal páramo complex.

The close relationship between human presence and peatland degradation is further reflected in the distribution of páramo settlements. The Eastern Cordillera contains a significant proportion of the population residing within páramo complexes (DANE, 2020), particularly in regions such as Tota - Bijagual - Mamapacha, Jurisdicciones-Santurbán-Berlín, Cruz Verde - Sumapaz, Pisba, Almorzadero, Guantiva - La Rusia, and Sierra Nevada del Cocuy. These páramos collectively support approximately 67% of the 80,000 people living in páramo ecosystems (DANE, 2020) and contain between 66 and 84% of all pasture peatlands identified in the study, reinforcing the link between human activity and peatland transformation. Notably, apart from Sumapaz, all these páramo complexes rank among the most affected, with over 20% of their peatlands converted into pasture.

Pasture peatlands occur where native vegetation is cleared or burned to create grazing areas for livestock and are often accompanied by hydrological alterations like drainage ditches to stabilize the soil. These alterations disrupt natural hydrology and accelerate peat decomposition and subsidence. Our mapping approach effectively identifies areas that remain wet but where native vegetation has largely been replaced by pasture. However, other degradation processes—such as ditching for water extraction, fires, and peat harvesting—also contribute to peatland loss but are not always detectable through land cover classification. Hydrological modifications, such as drainage ditches concealed by

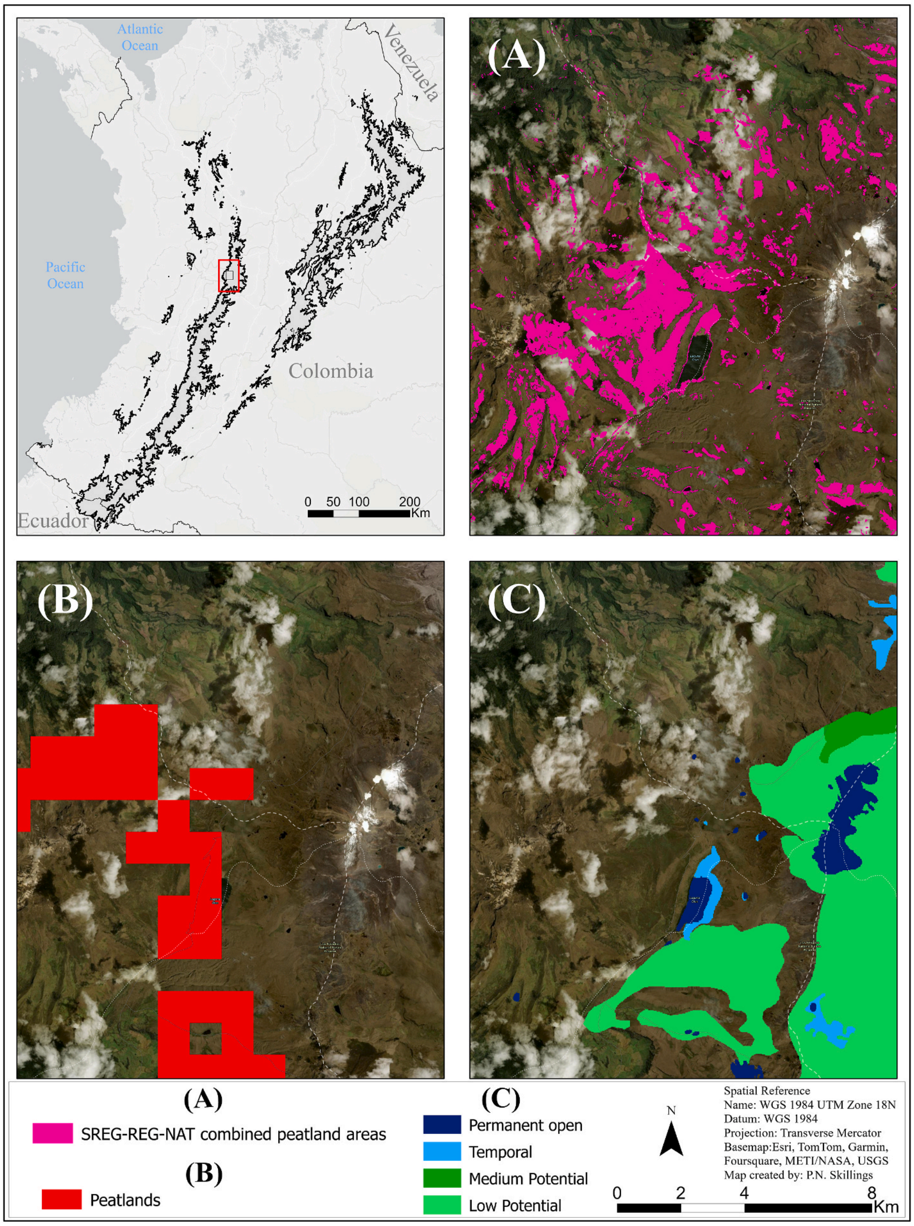

Fig. 7. Comparison of peatland and wetland maps in the National Natural Park Los Nevados. (A) Our combined peatland areas from SREG, REG, and NAT maps are shown in pink. (B) The Global Peatland Map 2.0 (GPM2) in red highlights its lower resolution, missing smaller peatlands. (C) The National Wetland Map of Colombia (NWMC) classifies wetlands with broad categories, including Permanent Open (blue), Temporal (light blue), and areas of Medium (green) and Low Potential (light green). This comparison shows the limitations of global and national maps in capturing detailed peatland distribution, underscoring the value of high-resolution mapping.

native vegetation, can remain undetected, as illustrated in Fig. 6(a and b). Even when natural vegetation is present, these hidden disturbances can severely impact peatland ecosystem function. Addressing these limitations in future studies will be critical, particularly as new methods for detecting drainage ditches and peatland degradation from fire continue to emerge (Carless et al., 2019; Lidberg et al., 2023; Robb et al., 2023; Sofan et al., 2019).

4.3. Peatland soil carbon

The carbon percentage (%C) and bulk density (BD) data in the top 40 cm may not accurately reflect the average conditions of peatland soils throughout their entire depth. Although our study only analyzed soil data up to 40 cm deep, full core analyses of mountain peatlands have provided a broader perspective. According to Hribljan et al. (2024), high BD (0.2–0.4 g cm-3) and low %C (15.4–31.6%) in páramo peatland soils are due to their high mineral content, a common characteristic of mountain peatlands. These peatlands are often found on mountainsides or valley bottoms, where steep eroding slopes can contribute significant alluvial, colluvial, or aeolian sediment, lowering %C and increasing BD (Hribljan et al., 2024). Additionally, mountain peatlands in volcanic regions receive considerable ash, further increasing the mineral content.

Peatlands have greater soil depths than any other land cover in the mountains (Chimner et al., 2023; Hribljan et al., 2016, 2024). The average depth of peatlands in the páramos of Colombia and Ecuador is estimated to be 442 cm, with an average total peatland carbon of 1628 Mg ha^{-1} (Hribljan et al., 2024). Scaling up these carbon estimates to the adjusted peatland areas from our national maps (Table 3), we estimated that peatland stocks in the mountains of Colombia contain between 366 and 407 Tg of carbon, which is 16–17 times more carbon per hectare in their soils than is contained in forest biomass in Colombia (Phillips et al., 2011). This translates to peat C equivalent of ~5% of national forest biomass C on 0.2% of the land area.

Hribljan et al. (2024) provides the most comprehensive dataset currently available for estimating carbon stocks in páramo peatlands across their total soil depth. However, there are important limitations to our current carbon stock calculations. A key constraint is the lack of accurate methods for determining peatland depth across the region. While the average carbon content per hectare from Hribljan et al. (2024) serves as a valuable proxy, it assumes an average peatland depth based on data from 16 cores in Ecuador and Colombia. Given the variability in peatland formation processes, hydrological conditions, and topographic settings, peat depth likely varies both within and across different peatland classes. Although this study uses the best available data, future research should prioritize understanding the spatial distribution of peatland depth, as this would enable more accurate and region-specific estimates of peatland soil carbon stocks.

It is worth noting that, although peatlands store the most soil C per unit area when considering the entire soil column to the base of the peatland, the soil C density of all ecosystems that we measured was quite substantial and roughly equivalent when only considering the top 40 cm of the soil (Supplementary Material-Tables S9-S11). According to the Colombia National Report on Soil Organic Carbon Sequestration Potential (Araujo-Carrillo, 2021), the Andean region is identified as the area with the highest potential to sequester CO_2, especially through improved management of croplands and grazing lands. Although the Colombia National Report does not mention peatlands, it highlights the importance of other Andean land covers for carbon stocks and carbon sequestration. They estimate that the Andean region possesses high contents of soil organic carbon stocks, often exceeding 100 Mg C ha^{-1} for soil depth up to 30 cm. This aligns with our soil carbon stocks result, which for all classes ranged from approximately 100 to 200 Mg ha^{-1} for the first 40 cm of soil depth (Supplementary Material-Table S11). Overall, the results show how valuable mountain ecosystems are for storing and sequestering carbon and help underscore the importance of management practices, such as water table management, peatland restoration, better agricultural practices, and upland reforestation, that can enhance their carbon sequestration potential.

4.4. Mapping mountain peatlands for conservation and climate mitigation

Mitigating peatland degradation requires a combination of conservation, restoration, and environmental education. The maps produced in this study serve as a crucial tool for identifying both conserved and degraded peatlands, helping local land managers, national park officials, and community leaders make informed decisions for sustainable management. These maps can guide conservation strategies by highlighting priority areas for peatland protection, ensuring that well-preserved peatlands continue to function as carbon sinks and water regulators. Establishing and enforcing conservation policies, such as restricting land conversion in critical peatland areas, can help prevent further disturbances.

Pasture peatlands identified in this study provide a key opportunity for targeted restoration efforts. By using the national-scale maps generated in this research, field exploration can be prioritized to assess the condition of potentially degraded areas and implement restoration where necessary. Restoration plays a key role in reversing degradation, particularly through rewetting drained peatlands and restoring hydrological conditions. These efforts have been shown to raise water tables, promote the recolonization of native vegetation, and enhance carbon sequestration in high-elevation peatlands, making them valuable strategies for climate change mitigation (Benavides-Duque and Hernández-Rodríguez, 2022; Planas Clarke et al., 2020; Suárez et al., 2022).

Equally important is environmental education, which fosters awareness of peatlands' ecological significance and promotes sustainable land-use practices. Future efforts should focus on making these maps accessible to local communities and developing workshops to increase awareness of peatland ecosystem services, particularly in remote areas where such knowledge remains limited. Community participation in restoration projects has demonstrated positive outcomes, as local populations develop a greater appreciation for peatlands and actively engage in their protection (Martínez-Amigo et al., 2022; Suárez et al., 2022). By integrating conservation, restoration, and education, stakeholders can leverage these peatland maps to enhance conservation planning and ensure the long-term sustainability of these critical ecosystems.

5. Conclusion

In this study, we developed the first comprehensive national-scale mountain peatland maps for Colombia, integrating advanced remote sensing and machine learning techniques. This research fills a key gap by providing the first comprehensive assessment of peatland extent, distribution, and transformation in the country. The methodologies and insights presented here are transferable to other tropical mountainous regions, contributing to global frameworks such as the Ramsar Convention. The mountain peatland national maps have significant implications for conservation planning and policy development, offering a foundation for targeted and effective strategies to protect and restore these critical ecosystems in Colombia.

Future research should focus on field validation in areas of identified discrepancies, improving peatland depth estimates, and integrating new remote sensing technologies to refine peatland mapping and detect other types of peatland degradation in Colombia. As the climate warms, local communities may increasingly rely on higher-elevation peatlands for water resources, potentially posing additional threats to these ecosystems. Increased disturbance is particularly concerning as tropical Andes peatlands store substantial soil carbon deposits that are highly sensitive to temperature changes (Hribljan et al., 2024), making them vulnerable to both warming and drainage.

The maps presented here mark a significant step toward understanding peatland distribution and condition in Colombia. Mapping peatland extent is fundamental for identifying opportunities for protection and sustainable management. As natural climate solutions, peatlands contribute to both climate adaptation and mitigation efforts. However, to fully understand peatland dynamics and inform effective conservation strategies, further research is needed to enhance resilience against climate change. This includes contributing to science-based policies aimed at protecting these carbon-rich ecosystems and maximizing their potential in climate adaptation and mitigation strategies.

CRediT authorship contribution statement

Patrick Nicolás Skillings-Neira: Writing – review & editing, Writing – original draft, Visualization, Validation, Supervision, Software, Project administration, Methodology, Investigation, Funding acquisition, Formal analysis, Data curation, Conceptualization. **Juan C. Benavides:** Writing – review & editing, Validation, Supervision, Resources, Project administration, Methodology, Funding acquisition, Conceptualization. **Michael J. Battaglia:** Writing – review & editing, Validation, Software, Methodology, Investigation, Data curation, Conceptualization. **Rodney A. Chimner:** Writing – review & editing, Writing – original draft, Validation, Supervision, Resources, Project administration, Methodology, Funding acquisition, Conceptualization. **Laura Bourgeau-Chavez:** Writing – review & editing, Validation, Software, Methodology, Data curation, Conceptualization. **Craig Wayson:** Writing – review & editing, Supervision, Project administration, Funding acquisition. **Randall Kolka:** Writing – review & editing, Supervision, Project administration, Funding acquisition. **Erik A. Lilleskov:** Writing – review & editing, Writing – original draft, Validation, Resources, Project administration, Methodology, Funding acquisition, Conceptualization.

Funding sources

This project was supported by the Sustainable Wetlands Adaptation and Mitigation Program (SWAMP), with additional financial assistance from the Society of Wetland Scientists Student Research Grant. The contents of this study are the sole responsibility of the authors and do not necessarily reflect the views of the United States Government.

Declaration of competing interest

The authors declare that they have no known competing financial interests or personal relationships that could have appeared to influence the work reported in this paper.

Acknowledgements

The authors acknowledge the support of Pontificia Universidad Javeriana and the Laboratory of Ecosystems and Climate Change. We greatly appreciate all the field work and lab analysis assistance of María Emilia Peláez, Alejandro Delgado, Ana María Rozo, Paola Alarcón, Carlos Ardila, Laura Báez, Andrés Becerra, Juan Esteban Botero, Natalia Cáceres, Sebastián Cortez, Juan Pablo Cantor, Santiago Mejía, Camila Merchán, Luisa Merchán, Sebastián Montero, Violeta Martínez, Camila Romero, Yeraldin Roa, Estefanía Ramírez, Santiago Rocha, Jorge Pérez, Silvio Ortegón, Mariana Ospino, Tatiana Rodríguez, Gina Santofimio, and Carlos Valbuena. Special thanks to Marcelo Villa for coding feedback, Ricardo Jaramillo and Esteban Suarez for field data from Ecuador, and Irene Aconcha for assistance with the research permit. We are grateful to National Natural Parks of Colombia, park rangers, local guides, and community leaders for their support.

Appendix A. Supplementary data

Supplementary data to this article can be found online at https://doi.org/10.1016/j.jenvman.2025.124915.

Data availability

All maps and related data from this research will be made publicly available on the SWAMP Dataverse platform (https://data.cifor.org/dataverse/swamp) in the near future.

References

Araujo-Carrillo, G.A., 2021. Colombia: soil organic carbon sequestration, potential national map national report, Version 1.0. http://hdl.handle.net/20.500.12324/37103.

Battaglia, M.J., Lafuente, A., Benavides, J.C., Lilleskov, E.A., Chimner, R.A., Bourgeau-Chavez, L.L., Skillings, P.N., 2024. Using remote sensing to map degraded mountain peatlands with high climate mitigation potential in Colombia's Central Cordillera. Front. Clim. 6, 1334159. https://doi.org/10.3389/fclim.2024.1334159.

Belgiu, M., Drăguţ, L., 2016. Random forest in remote sensing: a review of applications and future directions. ISPRS J. Photogrammetry Remote Sens. 114, 24–31. https://doi.org/10.1016/j.isprsjprs.2016.01.011.

Benavides, J., 2014. The effect of drainage on organic matter accumulation and plant communities of high-altitude peatlands in the Colombian tropical Andes. Mires Peat 15.

Benavides, J.C., Vitt, D.H., Cooper, D.J., 2023. The high-elevation peatlands of the northern Andes, Colombia. Plants 12 (4), 955. https://doi.org/10.3390/plants12040955.

Benavides-Duque, J.C., Hernández-Rodríguez, D.E., 2022. Páramos, humedales y bosques altoandinos. Experiencias de restauración para la mitigación del cambio climático en la alta montaña colombiana. Pontificia Universidad Javeriana. Programa Páramos y Bosques de USAID.

Bourgeau-Chavez, L., Endres, S., Battaglia, M., Miller, M.E., Banda, E., Laubach, Z., Higman, P., Chow-Fraser, P., Marcaccio, J., 2015. Development of a bi-national Great Lakes coastal wetland and land use map using three-season PALSAR and Landsat imagery. Remote Sens. 7 (7), 8655–8682. https://doi.org/10.3390/rs70708655.

Bourgeau-Chavez, L.L., Endres, S., Powell, R., Battaglia, M.J., Benscoter, B., Turetsky, M., Kasischke, E.S., Banda, E., 2017. Mapping boreal peatland ecosystem types from multitemporal radar and optical satellite imagery. Can. J. For. Res. 47 (4), 545–559. https://doi.org/10.1139/cjfr-2016-0192.

Bourgeau-Chavez, L., Endres, S.L., Graham, J., Hribljan, J.A., Chimner, R., Lillieskov, E., Battaglia, M., 2018. Mapping peatlands in boreal and tropical ecoregions. In: Liang, S. (Ed.), Comprehensive Remote Sensing, vol. 6. Elsevier, Oxford, UK, pp. 24–44. https://doi.org/10.1016/B978-0-12-409548-9.10544-5, 24–44.

Bourgeau-Chavez, L.L., Grelik, S.L., Battaglia, M.J., Leisman, D.J., Chimner, R.A., Hribljan, J.A., Lilleskov, E.A., Draper, F.C., Zutta, B.R., Hergoualc'h, K., 2021. Advances in Amazonian peatland discrimination with multi-temporal PALSAR refines estimates of peatland distribution, c stocks and deforestation. Front. Earth Sci. 9, 676748. https://doi.org/10.3389/feart.2021.676748.

Breiman, L., 2001. Random forests. Mach. Learn. 45, 5–32. https://doi.org/10.1023/A:1010933404324.

Carless, D., Luscombe, D.J., Gatis, N., Anderson, K., Brazier, R.E., 2019. Mapping landscape-scale peatland degradation using airborne lidar and multispectral data. Landsc. Ecol. 34, 1329–1345.

Castaño, C.U., Franco-Vidal, L., 2003. Colombia. In: Hofstede, R., Mena, V.P., Segarra, P. (Eds.), Los páramos del mundo: Proyecto Atlas Mundial de los Páramos. Global Peatland Initiative/NC-IUCN/EcoCiencia, pp. 39–85.

Castellanos, H.O., Gómez, W.F., Mayorga, N.C., 2021. Mapa nacional de coberturas de la tierra, escala 1:100.000, periodo 2018. Metodología Corine Land Cover adaptada para Colombia. Memoria Técnica Y Resultados.

Cataño Díaz, E.A., Uribe Meléndez, J., Campos Salazar, L.V., 2014. Diversidad hepáticas Y musgos en Turberas del nevado del tolima, Colombia. Caldasia. https://doi.org/10.15446/caldasia/v36n2.47479.

Chimner, R.A., Bourgeau-Chavez, L., Grelik, S., Hribljan, J.A., Clarke, A.M.P., Polk, M.H., Lilleskov, E.A., Fuentealba, B., 2019. Mapping mountain peatlands and wet meadows using multi-date, multi-sensor remote sensing in the Cordillera Blanca, Peru. Wetlands 39 (5), 1057–1067. https://doi.org/10.1007/s13157-019-01134-1.

Chimner, R.A., Resh, S.C., Hribljan, J.A., Battaglia, M., Bourgeau-Chavez, L., Bowser, G., Lilleskov, E.A., 2023. Mountain wetland soil carbon stocks of Huascarán National Park, Peru. Front. Plant Sci. 14, 1048609. https://doi.org/10.3389/fpls.2023.1048609.

Congalton, R.G., Green, K., 2019. Assessing the Accuracy of Remotely Sensed Data: Principles and Practices. CRC press. https://doi.org/10.1201/9780429052729.

Congreso de Colombia, 2018. Ley 1930 de 2018 - Por medio de la cual se dictan disposiciones para la gestión integral de los páramos en Colombia. Bogotá, Colombia: Diario Oficial No. 50.667 Retrieved from https://www.funcionpublica.gov.co/eva/gestornormativo/norma.php?i=87764.

Cooper, D.J., Kaczynski, K., Slayback, D., Yager, K., 2015. Growth and organic carbon production in peatlands dominated by Distichia muscoides, Bolivia, South America. Arctic Antarct. Alpine Res. 47 (3), 505–510. https://doi.org/10.1657/AAAR0014-060.

Cooper, D.J., Sueltenfuss, J., Oyague, E., Yager, K., Slayback, D., Caballero, E.M.C., Argollo, J., Mark, B.G., 2019. Drivers of peatland water table dynamics in the central Andes, Bolivia and Peru. Hydrol. Process. 33 (13), 1913–1925. https://doi.org/10.1002/hyp.13446.

Correa, A., Ochoa-Tocachi, B.F., Birkel, C., Ochoa-Sánchez, A., Zogheib, C., Tovar, C., Buytaert, W., 2020. A concerted research effort to advance the hydrological understanding of tropical páramos. Hydrol. Process. 34 (24), 4609–4627.

DANE, 2020. INFORME TÉCNICO CARACTERIZACIÓN POBLACIONAL ÁREAS DE PÁRAMO A PARTIR DE LOS RESULTADOS DEL CENSO NACIONAL DE POBLACIÓN Y VIVIENDA CNPV 2018.

Flórez-Ayala, C., Estupiñán-Suárez, L.M., Rojas, S., Aponte, C., Quiñones, M., Acevedo, Ó., Vilardy Quiroga, S.P., Jaramillo Villa, Ú., 2016. Identificación espacial de los sistemas de humedales continentales de Colombia. https://doi.org/10.21068/c2016s01a03.

Forkuor, G., Conrad, C., Thiel, M., Ullmann, T., Zoungrana, E., 2014. Integration of optical and synthetic aperture radar imagery for improving crop mapping in Northwestern Benin, west Africa. Remote Sens. 6 (7), 6472–6499. https://doi.org/10.3390/rs6076472.

Galvis, M.E., Avella, C., Sosa, C., Marín, C., Galvis, M., Victoria, M.I., Trujillo, M., 2021. Claves para la gestión local del páramo. Instituto de Investigación de Recursos Biológicos Alexander von Humboldt. http://hdl.handle.net/20.500.11761/35712.

Galvis Hernández, M., Ungar Ronderos, P.M., 2021. Páramos Colombia: Biodiversidad Y Gestión. Instituto de Investigación de Recursos Biológicos Alexander von Humboldt. http://hdl.handle.net/20.500.11761/35900.

Greifswald Mire Centre, 2022. Global peatland map 2.0. Underlying dataset of the UNEP global peatland assessment - the state of the world's peatlands: evidence for action toward the conservation, restoration, and sustainable management of peatlands, global peatlands initiative, united nations environment programme, nairobi. https://wedocs.unep.org/20.500.11822/37571.

Gumbricht, T., Roman-Cuesta, R.M., Verchot, L., Herold, M., Wittmann, F., Householder, J., Herold, N., Murdiyarso, D., 2017. An expert system model for mapping tropical wetlands and peatlands reveals South America as the largest contributor. Glob. Change Biol. 23. https://doi.org/10.1111/gcb.13689.

Gutiérrez-Díaz, J., Ordoñez-Delgado, N., Bolívar-Gamboa, A., 2020. Estimation of organic carbon in páramo ecosystem soils in Colombia. Ecosistemas. https://doi.org/10.7818/ECOS.1855.

Hofstede, R., Suárez Robalino, E., Mena-Vásconez, P., Calispa, M., Vásconez Paredes, F. J., Santamaría Freire, S.D., Samaniego Eguiguren, P., Mosquera, G.M., Ochoa-Sánchez, A.E., Pesántez Vallejo, J.P., 2023. Los páramos del Ecuador: Pasado, presente y futuro. UFSQ PRESS.

Hribljan, J., Cooper, D., Sueltenfuss, J., Wolf, E., Heckman, K., Lilleskov, E., Chimner, R., 2015. Carbon Storage and Long-Term Rate of Accumulation in High-Altitude Andean Peatlands of Bolivia.

Hribljan, J.A., Suárez, E., Heckman, K.A., Lilleskov, E.A., Chimner, R.A., 2016. Peatland carbon stocks and accumulation rates in the Ecuadorian páramo. Wetl. Ecol. Manag. 24 (2), 113–127. https://doi.org/10.1007/s11273-016-9482-2.

Hribljan, J.A., Suarez, E., Bourgeau-Chavez, L., Endres, S., Lilleskov, E.A., Chimbolema, S., Wayson, C., Serocki, E., Chimner, R.A., 2017. Multidate, multisensor remote sensing reveals high density of carbon-rich mountain peatlands in the paramo of Ecuador. Glob. Change Biol. 23 (12), 5412–5425. https://doi.org/10.1111/gcb.13807.

Hribljan, J.A., Hough, M., Lilleskov, E.A., Suarez, E., Heckman, K., Planas-Clarke, A.M., Chimner, R.A., 2024. Elevation and temperature are strong predictors of long-term carbon accumulation across tropical Andean mountain peatlands. Mitig. Adapt. Strategies Glob. Change 29 (1), 1. https://doi.org/10.1007/s11027-023-10089-y.

Jaramillo Villa, Ú., Flórez-Ayala, C., Cortés-Duque, J., Cadena-Marín, E.A., Estupiñán-Suárez, L.M., Rojas, S., Peláez, S., Aponte, C., 2016. Colombia anfibia. Un país de humedales, vol. I. Instituto de Investigación de Recursos Biológicos Alexander von Humboldt.

Krause, L., McCullough, K.J., Kane, E.S., Kolka, R.K., Chimner, R.A., Lilleskov, E.A., 2021. Impacts of historical ditching on peat volume and carbon in northern Minnesota USA peatlands. J. Environ. Manag. 296, 113090. https://doi.org/10.1016/j.jenvman.2021.113090.

Lazo, P.X., Mosquera, G.M., McDonnell, J.J., Crespo, P., 2019. The role of vegetation, soils, and precipitation on water storage and hydrological services in Andean Páramo catchments. J. Hydrol. 572, 805–819. https://doi.org/10.1016/j.jhydrol.2019.03.050.

Lidberg, W., Paul, S.S., Westphal, F., Richter, K.F., Lavesson, N., Melniks, R., Ivanovs, J., Ciesielski, M., Leinonen, A., Ågren, A.M., 2023. Mapping drainage ditches in forested landscapes using deep learning and aerial laser scanning. J. Irrigat. Drain. Eng. 149 (3), 04022051. https://doi.org/10.1061/JIDEDH.IRENG-9796.

Loisel, J., Yu, Z., Beilman, D.W., Camill, P., Alm, J., Amesbury, M.J., Anderson, D., Andersson, S., Bochicchio, C., Barber, K., 2014. A database and synthesis of northern peatland soil properties and Holocene carbon and nitrogen accumulation. Holocene 24 (9), 1028–1042.

Mahdianpari, M., Salehi, B., Mohammadimanesh, F., Brisco, B., Homayouni, S., Gill, E., DeLancey, E.R., Bourgeau-Chavez, L., 2020. Big data for a big country: the first generation of Canadian wetland inventory map at a spatial resolution of 10-m using Sentinel-1 and Sentinel-2 data on the Google Earth Engine cloud computing platform. Can. J. Rem. Sens. 46 (1), 15–33. https://doi.org/10.1080/07038992.2019.1711366.

Martínez-Amigo, V., Benavides-Duque, J.C., Hernández-Rodríguez, D.E., 2022. Restauración de humedales altoandinos: implementación de diseños para la mitigación del cambio climático. In: Benavides-Duque, J.C., Hernández-Rodríguez, D.E. (Eds.), Páramos, humedales y bosques altoandinos. Experiencias de restauración para la mitigación del cambio climático en la alta montaña colombiana. Pontificia Universidad Javeriana. Programa Páramos y Bosques de USAID, pp. 84–99.

Melton, J.R., Chan, E., Millard, K., Fortier, M., Winton, R.S., Martín-López, J.M., Cadillo-Quiroz, H., Kidd, D., Verchot, L.V., 2022. A map of global peatland extent created using machine learning (Peat-ML). Geosci. Model Dev. (GMD) 15 (12), 4709–4738. https://doi.org/10.5194/gmd-15-4709-2022.

Mosquera, G.M., Lazo, P.X., Célleri, R., Wilcox, B.P., Crespo, P., 2015. Runoff from tropical alpine grasslands increases with areal extent of wetlands. Catena 125, 120–128. https://doi.org/10.1016/j.catena.2014.10.010.

Olofsson, P., Foody, G.M., Stehman, S.V., Woodcock, C.E., 2013. Making better use of accuracy data in land change studies: estimating accuracy and area and quantifying uncertainty using stratified estimation. Rem. Sens. Environ. 129, 122–131. https://doi.org/10.1016/j.rse.2012.10.031.

Phillips, J., Duque, A., Yepes, A., Cabrera, K., García, M., Navarrete, D., Álvarez, E., Cárdenas, D., 2011. Estimación de las reservas actuales (2010) de carbono almacenadas en la biomasa aérea en bosques naturales de Colombia. Estratificación, alometría y métodos analíticos. Instituto de Hidrología, Meteorología, y Estudios Ambientales -IDEAM-, Bogotá D.C., Colombia, p. 68.

Planas Clarke, A.M., Chimner, R., Hribljan, J., Lilleskov, E., Fuentealba Durand, B., 2020. The effect of water table levels and short-term ditch restoration on mountain peatland carbon cycling in the Cordillera Blanca, Peru. Wetl. Ecol. Manag. 28, 51–69. https://doi.org/10.1007/s11273-019-09694-z.

Rangel-Ch, J., 2000. La región paramuna y franja aledaña en Colombia. In: Colombia diversidad biótica III: La región de vida paramuna. Universidad Nacional de Colombia. Editorial Unibiblos, Bogotá DC. Colombia, pp. 1–23.

Robb, C., Pickard, A., Williamson, J.L., Fitch, A., Evans, C., 2023. Peat drainage ditch mapping from aerial imagery using a convolutional neural network. Remote Sens. 15 (2), 499. https://doi.org/10.3390/rs15020499.

Roucoux, K.H., Lawson, I.T., Baker, T.R., Del Castillo Torres, D., Draper, F.C., Lahteenoja, O., Gilmore, M.P., Honorio Coronado, E.N., Kelly, T.J., Mitchard, E.T.A., Vriesendorp, C.F., 2017. Threats to intact tropical peatlands and opportunities for their conservation. Conserv. Biol. 31 (6), 1283–1292. https://doi.org/10.1111/cobi.12925.

Sarmiento Pinzón, C.E., Cortés-Duque, J., Suárez Mejía, A.P., 2013. Aportes a la conservación estratégica de los páramos de Colombia: actualización de la cartografía de los complejos de páramo a escala 1: 100.000.

Sofan, P., Bruce, D., Jones, E., Marsden, J., 2019. Detection and validation of tropical peatland flaming and smouldering using Landsat-8 SWIR and TIRS bands. Remote Sens. 11 (4), 465. https://doi.org/10.3390/rs11040465.

Soil Survey Staff, 2014. Soil survey field and laboratory methods manual. In: Soil Survey Investigations Report No. 51, Version 2.0. R. Burt and Soil Survey Staff. U.S. Department of Agriculture, Natural Resources Conservation Service.

Soil Survey Staff, 2015. Illustrated guide to soil taxonomy. US Department of Agriculture, Natural Resources Conservation Service, National Soil Survey Center: Lincoln, NE, USA 372.

Spagnuolo, O.S., Jarvey, J.C., Battaglia, M.J., Laubach, Z.M., Miller, M.E., Holekamp, K. E., Bourgeau-Chavez, L.L., 2020. Mapping Kenyan grassland heights across Large spatial scales with combined optical and radar satellite imagery. Remote Sens. 12 (7), 1086. https://doi.org/10.3390/rs12071086.

Suárez, E., Chimbolema, S., Jaramillo, R., Zurita-Arthos, L., Arellano, P., Chimner, R., Stanovick, J., Lilleskov, E., 2022. Challenges and opportunities for restoration of high-elevation Andean peatlands in Ecuador. Mitig. Adapt. Strategies Glob. Change 27 (4), 30. https://doi.org/10.1007/s11027-022-10006-9.

UNEP, 2022. Global Peatlands Assessment – the State of the World's Peatlands: evidence for action toward the conservation, restoration, and sustainable management of peatlands. Main Report. Global Peatlands Initiative. https://doi.org/10.59117/20.500.11822/41222.

Urbina, J.C., Benavides, J.C., 2015. Simulated small scale disturbances increase decomposition rates and facilitates invasive species encroachment in a high elevation tropical Andean peatland. Biotropica 47 (2), 143–151. https://doi.org/10.1111/btp.12191.

Villa, J.A., Mejía, G.M., Velásquez, D., Botero, A., Acosta, S.A., Marulanda, J.M., Osorno, A.M., Bohrer, G., 2019. Carbon sequestration and methane emissions along a microtopographic gradient in a tropical Andean peatland. Sci. Total Environ. 654, 651–661. https://doi.org/10.1016/j.scitotenv.2018.11.109.

Xu, J., Morris, P.J., Liu, J., Holden, J., 2018. PEATMAP: refining estimates of global peatland distribution based on a meta-analysis. Catena 160, 134–140. https://doi.org/10.1016/j.catena.2017.09.010.